UPPSALA
UNIVERSITET

Digital Comprehensive Summaries of Uppsala Dissertations from the Faculty of Science and Technology 1224

Distributed Photovoltaics, Household Electricity Use and Electric Vehicle Charging

Mathematical Modeling and Case Studies

JOAKIM MUNKHAMMAR

ACTA
UNIVERSITATIS
UPSALIENSIS
UPPSALA
2015

ISSN 1651-6214
ISBN 978-91-554-9162-8
urn:nbn:se:uu:diva-243159

Dissertation presented at Uppsala University to be publicly examined in Polhemsalen, Ångström Laboratory, Lägerhyddsvägen 1, Uppsala, Friday, 27 March 2015 at 13:15 for the degree of Doctor of Philosophy. The examination will be conducted in English. Faculty examiner: Professor Peter Lund (Aalto University).

Abstract

Munkhammar, J. 2015. Distributed Photovoltaics, Household Electricity Use and Electric Vehicle Charging. Mathematical Modeling and Case Studies. *Digital Comprehensive Summaries of Uppsala Dissertations from the Faculty of Science and Technology* 1224. 93 pp. Uppsala: Acta Universitatis Upsaliensis. ISBN 978-91-554-9162-8.

Technological improvements along with falling prices on photovoltaic (PV) panels and electric vehicles (EVs) suggest that they might become more common in the future. The introduction of distributed PV power production and EV charging has a considerable impact on the power system, in particular at the end-user in the electricity grid.

In this PhD thesis PV power production, household electricity use and EV charging are investigated on different system levels. The methodologies used in this thesis are interdisciplinary but the main contributions are mathematical modeling, simulations and data analysis of these three components and their interactions. Models for estimating PV power production, household electricity use, EV charging and their combination are developed using data and stochastic modeling with Markov chains and probability distributions. Additionally, data on PV power production and EV charging from eight solar charging stations is analyzed.

Results show that the clear-sky index for PV power production applications can be modeled via a bimodal Normal probability distribution, that household electricity use can be modeled via either Weibull or Log-normal probability distributions and that EV charging can be modeled by Bernoulli probability distributions. Complete models of PV power production, household electricity use and EV home-charging are developed with both Markov chain and probability distribution modeling. It is also shown that EV home-charging can be modeled as an extension to the Widén Markov chain model for generating synthetic household electricity use patterns. Analysis of measurements from solar charging stations show a wide variety of EV charging patterns. Additionally an alternative approach to modeling the clear-sky index is introduced and shown to give a generalized Ångström equation relating solar irradiation to the duration of bright sunshine.

Analysis of the total power consumption/production patterns of PV power production, household electricity use and EV home-charging at the end-user in the grid highlights the dependency between the components, which quantifies the mismatch issue of distributed intermittent power production and consumption. At an aggregate level of households the level of mismatch is shown to be lower.

Keywords: Distributed Photovoltaics, Household Electricity Use, Electric Vehicle Charging, Markov Chain Modeling, Probability Distribution Modeling, Data Analysis, Self-Consumption, Grid Interaction.

Joakim Munkhammar, Department of Engineering Sciences, Box 534, Uppsala University, SE-75121 Uppsala, Sweden.

© Joakim Munkhammar 2015

ISSN 1651-6214
ISBN 978-91-554-9162-8
urn:nbn:se:uu:diva-243159 (http://urn.kb.se/resolve?urn=urn:nbn:se:uu:diva-243159)

If my calculations are correct,
when this baby hits 88 miles per hour...
you're gonna see some serious shit.

Dr. Emmett Brown,
Back to the future (1985)

This thesis is based on work conducted within the interdisciplinary graduate school Energy Systems. The national Energy Systems Programme aims at creating competence in solving complex energy problems by combining technical and social sciences. The research programme analyses processes for the conversion, transmission and utilisation of energy, combined together in order to fulfil specific needs.

PROGRAM
ENERGISYSTEM
Forskning och forskarskola

The research groups that participate in the Energy Systems Programme are the Department of Engineering Sciences at Uppsala University, the Division of Energy Systems at Linköping Institute of Technology, the Department of Technology and Social Change at Linköping University, the Division of Heat and Power Technology at Chalmers University of Technology in Göteborg as well as the Division of Energy Processes at the Royal Institute of Technology in Stockholm.

www.liu.se/energi

List of papers

This thesis is based on the following papers, which are referred to in the text by their Roman numerals.

I **Munkhammar, J.**, Rydén, J., Widén, J., Lingfors, D., Simulating dispersed photovoltaic power generation using a bimodal mixture model of the clear-sky index, manuscript 2014.

II **Munkhammar, J.**, Widén, J., On a Probability Distribution Convolution Approach to Clear-Sky Index and a Generalized Ångström Equation, manuscript 2014.

III **Munkhammar, J.**, Rydén, J., Widén, J., Characterizing probability density distributions for household electricity load profiles from high-resolution electricity use data, Applied Energy 2014: 135; 382-390.

IV Grahn, P., **Munkhammar, J.**, Widén, J., Alvehag, K., Söder, L., PHEV Home-Charging Model Based on Residential Activity Patterns, IEEE Transactions on Power Systems 2013: 28; 2507-2515. © 2013 IEEE.

V **Munkhammar, J.**, Grahn, P., Rydén, J., Widén, J., A Bernoulli Distribution Model for Plug-in Electric Vehicle Charging based on Time-use Data for Driving Patterns, in Proceedings of IEEE International Electric Vehicle Conference (IEVC2014) in Florence, Italy, 17-19 December 2014. © 2014 IEEE.

VI **Munkhammar, J.**, Bishop, J.D.K., Sarralde, J. J., Tian, W., Choudhary, R., Household electricity use, electric vehicle home-charging and distributed photovoltaic power production in the city of Westminster, Energy and Buildings 2014: 86; 439-448.

VII **Munkhammar, J.**, Grahn, P., Widén, J., Quantifying self-consumption of on-site photovoltaic power generation in households with electric vehicle home charging, Solar Energy 2013: 97; 208-216.

VIII **Munkhammar, J.**, Rydén, J., Widén, J., On a probability distribution model combining household power consumption, electric vehicle home-charging and photovoltaic power production, Applied Energy 2015: 142; 135-143.

IX **Munkhammar, J.**, Widén, J., Wickman, P., Electric Vehicle Charging and Photovoltaic Power Production from Eight Solar Charging Stations in Sweden, in Proceedings of 4th International Workshop on Integration of Solar into Power Systems in Berlin, Germany, 10-11 November 2014; 425-429.

Reprints were made with permission from the publishers.

Publications not included in the thesis

X Widén, J., Karresand, H., Küller, A., Liu, L., **Munkhammar, J.**, Thoresson, J., Åberg, M., Forskningssyntes för konsortiet byggnader i energisystem, 2015.

XI Helbrink, J., Linnarsson, J., Lindén, M., Edfeldt, E., Pogosjan, D., **Munkhammar, J.**, Grahn, P., Krav på framtidens elnät - smarta elnät, North European Power Perspectives report (Sweco) 2014.

XII Damsgaard, N., Lindén, M., Yuen, K., Helbrink, J., Andersson M., Einarsson, M., **Munkhammar, J.**, Grahn, P., Framtida krav på elnäten, Elforsk report 14:26, 2014.

XIII Ackeby, S., Bollen, M., **Munkhammar, J.**, Prosumer with demand-response: Distribution network impact and mitigation, Elforsk report 13:59, 2013.

XIV **Munkhammar, J.**, Widén, J., Nilsson, A., Photovoltaic Potential of Alternative Year-Round Daylight Savings Time, in Proceedings of 28th European PV Solar Energy Conference (EU-PVSEC) in Paris, France, 30 September - 4 October 2013.

XV Widén, J., **Munkhammar, J.**, Evaluating the benefits of a solar home energy management system: Impacts on photovoltaic power production value and grid interaction, in Proceedings of the European Council for Energy Efficient Economy (ECEEE) 2013 Summer Study, Presqu'île de Giens, France, June 3-8, 2013.

XVI **Munkhammar, J.**, Markov-chain modeling of energy users and electric vehicles: Applications to distributed photovoltaics, Licentiate thesis, Uppsala University 2012.

XVII **Munkhammar, J.**, Widén, J., A stochastic model for collective resident activity patterns and energy use: preliminaries, in Proceedings of Sustainability in Energy and Buildings (SEB) Stockholm, Sweden, 3-5 September 2012.

XVIII **Munkhammar, J.**, Widén, J., A flexible Markov-chain model for simulating demand side management strategies - applications to distributed photovoltaics, in Proceedings of the World Renewable Energy Forum (WREF) May 13-17 in Colorado, USA, 2012.

XIX Hellgren, M., Grahn, P., **Munkhammar J.**, Photovoltaics, electric vehicles and energy users: A case study of the Royal Seaport - Visions and energy user expectations, Working paper no. 50, Energy Systems Programme, Linköping University 2011.

XX Widén, J., **Munkhammar, J.**, Widespread integration of distributed photovoltaics at high latitudes: opportunities and challenges, in conference proceedings of European PV Solar Energy Conference (EU-PVSEC) in Hamburg, Germany, 5-9 September 2011.

XXI **Munkhammar, J.**, Chaos in a fractional order logistic map, Fractional Calculus and Applied Analysis 2013: 16; 511-519.

XXII **Munkhammar, J.**, Canonical Relational Quantum Mechanics from Information Theory, Electronic Journal of Theoretical Physics 2011: 8; 93-108.

XXIII Mattsson, L., **Munkhammar, J.**, Runaway growth of fractal dust grains, in F. Kerschbaum, J. Hron, and R. F. Wing, eds, to appear in Conference Series, Why Galaxies care about AGB Stars III, Astronomical Society of the Pacific, San Francisco, 2015.

XIV Mattsson, L., Andersen, A. C., **Munkhammar, J.**, On the dust abundance gradients in late-type galaxies: I. Effects of destruction and growth of dust in the interstellar medium, Monthly Notices of the Royal Astronomical Society 2012: 423, 26-37.

Notes on my contribution to the appended papers

- *Paper (I)* — Initiated the project, devised and developed most of the model together with Jesper Rydén and Joakim Widén, did most simulations and writing.

- *Paper (II)* — Initiated the project, devised and developed most of the model together with Joakim Widén, did all simulations and most of the writing.

- *Paper (III)* — Initiated the project, devised and developed most of the model together with Jesper Rydén and Joakim Widén, did all simulations and most of the writing.

- *Paper (IV)* — Co-initiated the project and co-developed the model with Pia Grahn and assisted in writing.

- *Paper (V)* — Initiated the project, devised and developed most of the model together with Pia Grahn, Jesper Rydén and Joakim Widén, did all simulations and writing.

- *Paper (VI)* — Initiated the project, devised and performed most of the simulations, except UKmap estimates, and did most of the writing.

- *Paper (VII)* — Initiated the project, did all simulations and most of the writing.

- *Paper (VIII)* — Initiated the project, did all model development, all simulations and most of the writing.

- *Paper (IX)* — Did all data analysis and most of the writing.

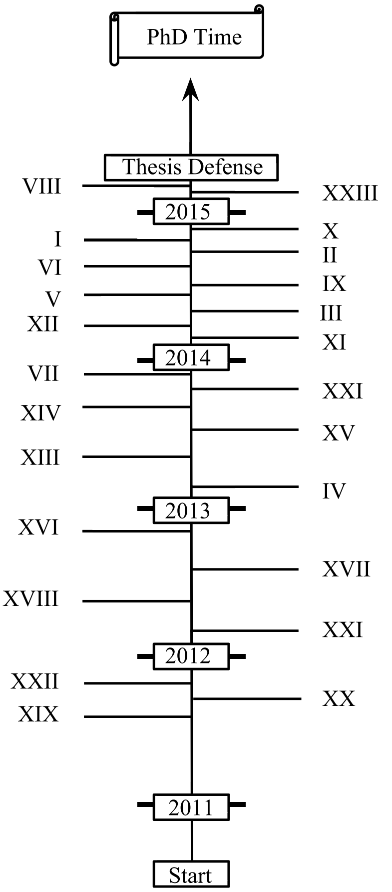

Figure 1. A schematic illustration representing dates of publication for all publications (appended or not) during the PhD-project. For the unpublished manuscripts (I) and (II), the finish dates are given instead.

Contents

Nomenclature

BHI	Beam Horizontal Irradiance
CDF	Cumulative Distribution Function
DHI	Diffuse Horizontal Irradiance
DoD	Depth of Discharge
EM	Expectation Maximization
EV	Electric Vehicle
GHI	Global Horizontal Irradiance
GO:s	Guarantees of Origin
HEV	Hybrid Electric Vehicle
ICE	Internal Combustion Engine
K-S	Kolmogorov-Smirnov
NZEB	Net-Zero Energy Building
PDF	Probability Density Function
PEV	Plug-in Electric Vehicle
PHEV	Plug-in Hybrid Electric Vehicle
PMF	Probability Mass Function
PV	Photovoltaic/Photovoltaics
SOC	State Of Charge
TUD	Time-Use Data

1. Introduction

During the time before the industrial revolution people had to deal with poverty, starvation and generally bad living conditions. Life expectancy and working conditions were immensely bad compared with today's standards. Even the richest during those times — such as the kings — did not have access to modern day dentistry or simple medications such as antibiotics, which led to misery and suffering compared with even the most modest of today's standards in the western world. The industrial revolution brought on tremendous improvements for people in the world by providing better food and curing deceases.

Technological advances enabled increased prosperity by more effectively utilizing resources. The primary function of the revolution was not a redistribution of the wealth — but rather the enabling of the development of specializations and innovations which in turn led to more efficient and diverse production of goods and services by utilizing synergy. These processes of industrialization are today present — where not hindered — in developing countries. The total GDP of the world increased nearly 50 times from 1820 to 1998 [1, p.28] which indicates that the development of the world is dynamic and not a zero-sum game. As a result of the industrial revolution societal systems in the industrialized nations grew in prosperity, size and complexity which required more energy to sustain their processes.

The historically rapid improvement in global prosperity through economic and technological development has apart from synergistic accomplishments also led to challenges associated with changing ecosystems, increased CO_2 emissions and resource depletion. Since prosperity is necessary for the survival of life on Earth there is a continued need for human development and a key feature in resolving these issues is technological advancement [2].

The primary necessity for upholding and advancing human societies lies in the ability to harness a reliable and abundant source of power. Today all energy sources — except nuclear, geothermal and tidal power — have their origin in solar radiation. The crucial problem is how to utilize this irradiated solar energy. Coal and oil are solar radiation energy stored over long time during earlier epochs of the Earth's history. Wind power obtains its energy from the weather system — which in turn is driven by solar radiation. Hydro power is energy from reservoirs that have been filled by rain, biofuel is derived from plants that have absorbed solar radiation and via photosynthesis. Despite modern PV cells having a typical efficiency of about 16 percent they are still the most efficient utilisers of the sun's radiation per unit area [3].

Although coal and oil are naturally replenished energy sources they are not considered renewable due to the long time-scale on which they are renewed.

The Earth is radiated by about 800 million TWh annually which is 10,000 times more than is necessary to match the global energy demand for a year [4, p.13]. In terms of the time-scale of renewability photovoltaic power delivers an instantaneous production of electricity when irradiance is present. Despite these favorable features there are challenges for the large-scale development of photovoltaic power production in the world. In particular this is true at high latitude regions such as Sweden, with high seasonal variability in solar irradiance.

There is no significant economy of scale of a PV system, hence making large-scale centralized PV power plants no more feasible than local distributed PV [5, p.32]. Considering costs associated with pole mounts and foundation mounts for PV systems this makes existing building rooftops and façades interesting. Residential buildings are particularly interesting because of the proximity to the end-user in the grid along with the total nationwide rooftop availability. Installing PV systems on a household level has become interesting from an economic perspective, especially when the PV system is grid-connected. Indeed, due to falling PV module prices and the aid of governmental subsidies for installing PV-systems as well as generous feed-in tariffs the market for distributed PV has increased considerably since the turn of the millennium.

Large amounts of installed PV as distributed generation has further pushed for the need to modernize and redesign the power system into a so-called smart grid. Such systems aim to utilize information regarding electricity consumer and producer behavior in order to improve efficiency, reliability, economics and sustainability of the production and distribution of electricity [6]. The design and operation of a smart grid is then dependent on the variability of load and electricity production over time for different locations in the grid.

The injection of PV power into the grid at the end-user should not surpass the so-called hosting capacity of the grid, that is when voltages or loading of components and losses in the grid reach unacceptable levels [7, p.89]. For Swedish conditions hosting capacities were found to be the highest for city grids, followed by suburban and rural grids [8]. Given no local energy storage in the household the proximity of load and power production is mostly beneficial if the load is matched with the production.

In this context of PV power self-consumption local EV charging is interesting. Since the number of plug-in EVs in the world is expected to increase it is of particular interest to investigate the coincidence between PV power production and EV charging. Generally electrification of transportation represents a significant potential for energy efficiency worldwide, and when connected to renewable energy sources an even greater reduction of fossil fuel use is achieved. In similarity with PV power production EV charging has an impact on the power system when introduced. This means that quantifying EV charging over time — like PV power production — is of interest for power system design and operation.

In general, to sum up, characterizing instantaneous PV power production, household electricity use, EV charging and their combination is necessary for the design and operation of future electricity grids and for the facilitation of efficient energy use.

1.1 Aim of the thesis

The work presented in this thesis is the outcome of a PhD-project for in-depth interdisciplinary investigations regarding distributed PV power production, household electricity use and EV charging. This PhD project was carried out within the Energy Systems Programme, a national research programme and graduate school aimed at interdisciplinary research concerning energy systems. The research questions addressed within this project concern challenges and opportunities with distributed PV power production, household electricity use and EV charging. The overall aim is to develop models for PV power production, household electricity use and EV charging that can be used to quantify grid interaction and self-consumption. The study has the following more specific aims, which are addressed in the appended papers:

- *Develop mathematical models for solar irradiance and PV power production* (Papers I-II).
- *Develop a mathematical model for household electricity use* (Paper III).
- *Develop mathematical models for EV charging* (Papers IV-V).
- *Develop, investigate and apply mathematical models regarding the combined system of PV power production, household electricity use and EV charging to study grid interaction and self-consumption* (Papers VI-VIII).
- *Investigate and analyze grid interaction and self-consumption from meter data on PV power production and EV charging* (Paper IX).

1.2 Overview of appended papers

This thesis is composed of papers based on interdisciplinary research collaborations. The results are based on the appended papers listed below. An overview of methods and applications in the papers is included in Table 1.1.

- *Paper I* presents a probability distribution model for PV power production based on solar irradiance data for Norrköping, Sweden. A bimodal Normal probability distribution model for clear-sky index is developed and combined with a PV power production model. The model estimates solar irradiance variability and PV power production for arbitrarily orientated surfaces for single locations and introduces an approximate model for PV power production based on an aggregate clear-sky index for multiple locations.

- *Paper II* introduces an approach to solar irradiance modeling via the process of convolution of probability distributions which results in a generalized Ångström equation relating solar irradiance to duration of sunshine over time.

- *Paper III* presents Weibull and Log-normal probability distribution models for household electricity use based on data on Swedish household electricity use from the Swedish Energy Agency. These models are developed primarily for simulating the individual household level, but investigations of multiple uncorrelated households are also included.

- *Paper IV* presents a model of EV home-charging as an extension to the Widén Markov chain model for household electricity use developed in [9]-[10].

- *Paper V* presents a Bernoulli probability distribution model for EV charging based on time-use data on Swedish travel behavior. The model assumes charging at each stop and simulates city driving with a maximally developed charging infrastructure. Investigations on aggregates of EV charging is also presented.

- *Paper VI* presents a case study for the City of Westminster (London, UK) of PV power production, household electricity use and EV home-charging. PV power production was estimated from solar irradiance and a model developed in [5]. The household electricity use was obtained from the Widén Markov chain model, developed in [9]-[10], and the EV charging was obtained from the Markov chain model for EV charging developed in paper (IV). This project was carried out in collaboration with the Energy Efficient Cities Initiative at Cambridge University.

- *Paper VII* presents a study regarding self-consumption of PV power production from household electricity use and EV home-charging. This paper is based on PV power production data from the Ångström Laboratory, and household electricity use from the Markov chain model developed in [9]-[10]. The EV home-charging model was developed in paper

(IV).

- *Paper VIII* introduces a probability distribution model for PV power production, household electricity use and EV home-charging based on the probability distribution models developed in papers (I), (III) and (V). This model is used to quantify the correlation between electricity load and PV power production at for individual households and for aggregates of households.

- *Paper IX* quantifies PV power production and EV charging meter data from eight solar charging stations distributed across Sweden. The solar charging stations and data was provided by Solelia Greentech AB.

Table 1.1. *Methodology(ies) for each studied component in the appended papers.*

	Markov chain	Distribution	Data analysis
Photovoltaics	—	(I), (II), (VIII)	(IX)
Household electricity use	(IV),(VI),(VII)	(III), (VIII)	—
Electric vehicles	(IV), (VI), (VII)	(V), (VIII)	(IX)

2. Background

In this chapter the general background for the research in this thesis is presented. An introduction to system theory and power systems research is given in Section 2.1 and a background to distributed generation and the power system is given in Section 2.2. The background on PV technology and PV power production is presented in Section 2.3, and the background on household electricity use is presented in Section 2.4. Finally the background on EV technology and EV charging is presented in Section 2.5. The chapter is concluded with identified research gaps in Section 2.6.

2.1 Systems theory

Interdisciplinary research has, in addition to research depth, also a research width since it covers several traditional fields of research. In such research it is particularly important to delimit projects by means of identifying and quantifying systems with clearly defined limits. This can to some extent be addressed by systems theory.

There are many types of systems such as physical systems, biological systems, social systems and power systems. Despite having different content systems often have many aspects in common, such as basic underlying structures and rules. There exist principles, rules and models which are universal and can be found in many systems. Regardless of area of application these principles or rules are often formulated by mathematics, take for example the width in application of probability distribution modeling in papers (I),(II),(III),(V),(VIII) and (XXII)-(XXIII). Bertalanffy defined *General Systems Theory* as a subject matter of formulation and derivation of principles which are valid for systems in general [11, p.31]. In that sense systems theory can be seen as an interdisciplinary theory of how systems work in a general context. In many ways a system can be seen as a set of components which together constitute a complex structure [12].

The research in this thesis regards several kinds of systems, where the system setup for each study is necessarily dependent on the aim of that particular project. The concept of system levels can assist in classifying this from a system perspective. When studying PV power production the outermost system limit is the solar system, and for most current applications the sun-earth system.

Within this system it is instructive to first imagine the fusion-based production of electromagnetic radiation in the sun's interior, the radiative transport through the different layers of the sun. Further on the system limit is narrowed down to include radiative transport through the Earth's atmosphere where it is attenuated by absorbtion, emission and reflection. Then finally the system limit surrounds the interactions of the incoming photons with the electrons in the semi-conductor material in the PV panels. In turn this expands the system limit to include societies which enable human control of solar energy in terms of produced and accessible electric power. An increased coverage of PV panels in the world increases the total solar power that is harnessed by humans, and for studies of PV power production the system limit expands. Finally it can reach an upper limit of maximization — an outer system limit for solar energy — corresponding to a hypothetical so-called Dyson sphere, which is a proposed megastructure where the sun is completely covered with PV panels [13].

For most studies simplifying assumptions are applied, which represent system limits in an abstract sense. Take for example household electricity use. It is to a large extent dependent on the daily activities of residents in combination with available appliances. EV use and charging is also dependent on human behavior, where delimiting assumptions often regard setup on EVs, charging stations and route planning. PV power production is also based on delimiting assumptions regarding for example atmospheric conditions. But regardless of study there are often common grounds for interaction between sub-systems. For example a study involving PV power production, household electricity use and EV charging have common grounds of interaction such as diurnal and seasonal variations in weather and temperature, which affect all three components, albeit in different ways. A schematic illustration of investigated systems in this thesis is shown in Figure 2.1.

A key issue in devising projects for determining the interrelation between these — or any generally interacting — systems is then to define system limits in such a way that the interaction is maximally quantified whilst extraneous information is minimized. This suggested "interdisciplinary research optimum" perhaps qualifies as a representative of a proposed optimal junction between principle-based theory and a pragmatic approach [14].

Figure 2.1. A system-based schematic illustration of a house, a resident, an electric vehicle and a photovoltaic system which in essence constitutes the systems investigated in this thesis.

2.2 Distributed generation in the power system

In this section the Swedish power system and distributed PV power production are reviewed.

2.2.1 The Swedish power system and distribution grid

Power systems have been described as the most complex systems ever created and operated by humans [15, p.139]. Historically in Sweden — in the late 19th century — electric power production was local. In Sweden the transition was often made from old hydro-powered mills to hydro power plants [16]. In those places where a hydro power plant could not be constructed a coal power plant was built instead. As the technology for transmission and distribution of electric power was developed the possibility for establishing centralized power production was enabled. The use of alternating current made it possible to first construct regional grids and eventually a national system [16].

The current energy mix in the grid in Sweden consists of mostly hydro power and nuclear power, but with a growing fraction of renewable energy. The renewable electricity production, other than hydro power, is dominated by wind power [17]. In 2013 the total wind power production was estimated at 10 TWh, which was a 7 percent share of the total electricity production in Sweden. PV provides a small contribution in Sweden with an installed power of 43.1 MW_p — or a 0.03 percent of total annual electricity production — at the end of 2013 [18].

The Swedish transmission and distribution grid can be divided into three major levels. The national level has a 400 kV or 220 kV, which is distributed to regional grids where it is transformed to 30-130kV [19, 20]. In turn this is transformed to 10 kV in the distribution grid [19]. From there substations transform it to 400 V which is distributed at the household level [19]. Distributed generation can be injected into any level of the electricity grid. The grid-connected PV power production In this thesis the PV power production is primarily assumed to be injected at the household level.

2.2.2 Challenges with distributed generation

Distributed generation stands in contrast to centralized generation by being injected at various different locations and levels in the electricity grid. It is also potentially without centralized operation and control. This means that an increased introduction of distributed generation in the power system increases the complexity of the system. There are basically two different challenges with distributed generation, which is particularly important when dealing with intermittent power generation such as PV.

On the one hand, with large amounts of intermittent power production there is an increased need for power system balancing to keep the system frequency within limits. On the other hand, which is most relevant for this thesis, the local distribution grid may experience new, reversed, power flows, voltage rises and component overloading. Voltage disturbances include reduction of equipment lifetime, erroneous tripping of the equipment, and damage to equipment [7, p.92]. This calls for advanced power system control when large quantities of intermittent power generators such as PV are connected at the end-user in the grid [15, p.139].

The challenge for distributed generation is that the distribution grid has limits regarding the amount of power which may be injected at the end-user site. Hosting capacity is defined as the amount of distributed generation for which the performance becomes unacceptable [7, p.89]. It is measured for example as a fraction of injected power compared with the load on an annual basis [8]. It is a performance index which is suitable to use as power quality indicator regarding issues such as voltage rise, overloading and harmonics. As an example it was determined that the hosting capacity in Sweden was 60% for rural and suburban grids while for a city grid it could be as high as 325% [8].

2.2.3 Renewable energy

Modern distributed generation such as PV is often based on sources of renewable energy. For a modern society the production of electric power is necessary for providing a decent life for any citizen, which means that if many options for electric power production are available then there is usually a preference relation among these options. In face of possible abundance limitations of fossil fuel combined with potential environmental problems related to their combustion considerable amount of attention has been given to the field of renewable energy sources [21]. The definition of renewable energy sources is the following according to Encyclopedia Britannica [22]:

> Renewable energy is usable energy derived from replenishable sources such as the sun (solar energy), wind (wind power), rivers (hydroelectric power), hot springs (geothermal energy), tides (tidal power), and biomass (biofuels).

Today most electricity production in the world comes from non-renewable energy sources where fossil fuels constitute 78.4 percent, nuclear 2.6 percent and renewables 19.0 percent [21, p.21]. Among the renewable energy sources PV has expanded considerably during the last decade. Most of the installed PV power is in the International Energy Agency Photovoltaic Power System Programme (IEA-PVPS) countries, where the biggest producers are Germany and Italy [23, p.39]. The cumulative installed PV power in the world is shown in Figure 2.2.

The overwhelming majority of the installed PV systems are grid-connected and connected at the very lowest voltage level of the distribution grid [23, p.14].

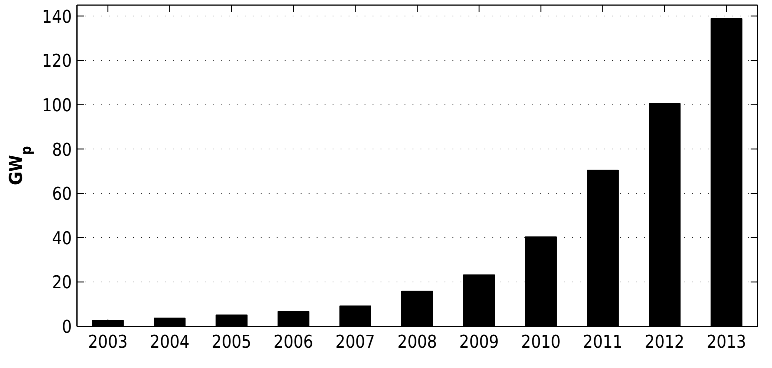

Figure 2.2. Global cumulative installed PV peak power between 2003 and 2013 [24, p.17].

2.3 Solar irradiance and photovoltaics

This section reviews photovoltaic technology, its applications and challenges with integration in the power system.

2.3.1 Photovoltaic technology

The common consensus when speaking of active solar energy is that it regards direct conversion from solar radiation into heat and/or electricity [15, p.61].

In this category PV is a special case since it directly converts the energy from incoming solar photons into a current using semiconductor materials [25, p.4]. In terms of physics solar cell technology is based on the photovoltaic effect first reported by Bequerel in 1839 [25]. The function of each photovoltaic cell is to absorb the incoming photons which then frees electrons via charge separation in the absorbing material [15, p.62]. This in turn generates a voltage in the material, which in a circuit generates an electric current. In 2013 silicon-wafer based PV technology accounted for about 90 % of the total production in the world [26, p.4].

Depending on size and efficiency these modules typically range from a few watts up to some 100 watts, hence PV systems have a wide range in size from pocket calculators to parks of PV arrays. Current silicon PV modules have a typical efficiency of about 16 percent and the world record for high-concentration multi-junction solar cells is 44.7 percent [26, p.6]. One example of a PV module, which was analyzed in terms of power production in paper (IX), is the Yingli 240p-29b based on polycrystalline technology with 14.7 percent efficiency and a peak power of 240 W_p [27]. An example of a park of solar-tracking PV arrays is shown in Figure 2.3.

Figure 2.3. A park of solar-tracking PV arrays in Västerås, Sweden. Photo: Joakim Munkhammar 2014.

The output of power from photovoltaic systems depends on the setup of the particular photovoltaic system used. Latitude and tilting of planes are examples of important variables for the setup of a photovoltaic system, which will be discussed in detail in Section 3.2.5. In Figure 2.4 simulated daily average PV power production over a year for an 81 m^2 PV array located at Uppsala, Sweden, is given along with an example of a simulated average daily load profile from one-year household electricity use.

2.3.2 Photovoltaic power production

PV power production is generally classified into being either stand-alone or grid-connected [23], of which the overwhelming majority of installations today are grid-connected [23, p.14]. The total installed PV power capacity in the world was in 2013 nearly 140 GW_p as was shown in Figure 2.2 along with a ten year trend of development. Potentially large amounts of PV power production injected into the grid at the end-user could cause problems if it exceeds the hosting capacity. In order to avoid costly grid-reinforcements there are essentially three main methods for increasing the hosting capacity for PV: adjusting tap changer settings at the transformer substation, PV inverter active power curtailment and reactive power control [8]. It was shown that the most effective options for dealing with over voltages during limited time intervals and narrow control ranges was reactive power control and curtailment [8]. During times of high-load adjusting tap changers lowered all voltages, not just the critical ones [8, p.7]. Another way to circumvent the problem of insufficient hosting capacity is to increase the self-consumption of the PV power to lower the power injected into the grid.

2.3.3 Photovoltaic power self-consumption

Based on data and model estimates the coincidence between PV power production and household electricity use is generally suboptimal [28, p.1953]. In particular this regards countries at high latitudes, such as Sweden, where household electricity demand and PV electricity production are negatively correlated both on annual and diurnal basis [28, p.1953]. As a way of illustrating this mismatch an example of a daily average household electricity use profile is given along with a PV power production profile in Figure 2.4.

The importance of increasing the hosting capacity by increasing the level of self-consumption of PV power was mentioned previously. There are emerging technologies that integrate PV systems with energy storage systems mainly as a means to increase the level of self-consumption [29, 30, 31, 32]. Even tariffs favorable for self-consumption have been implemented [23]. Self-consumption is particularly interesting for countries with a mature PV market such as Germany where feed-in tariffs have declined. Studies on battery storage as a means to increase self-consumption also point to the need for improved technology and demand-side management [30, 33, 34]. There are new technological solutions which help to improve the self-consumption, such as the "Sunny Home Manager" from SMA [32]. Self-consumption of PV power has been investigated in connection with net-zero energy buildings (NZEBs) in for example [35], and EV charging in [36]. Another study shows the impacts of various options for obtaining a lower mismatch between production and consumption [28]. That study focused on the following three possible options: PV array orientation, demand side management and electrical storage. Electrical

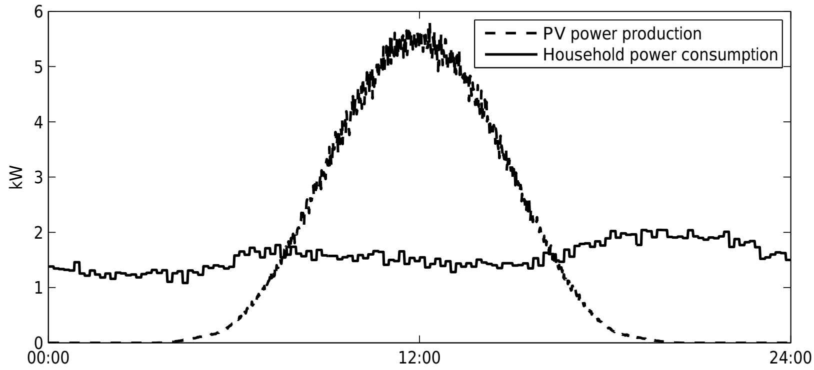

Figure 2.4. Year-average daily PV power production (dashed) and household load (solid) are given. The household load is represented by synthetic load generated from the Weibull probability distribution model developed in paper (III). The PV power production is synthetically generated by the PV power production probability distribution model developed in paper (I), for location Uppsala, Sweden (59° 50'19" N 17° 38'50" E). The simulated PV system is sized up for annual net-zero energy with an 81 m^2 PV system facing south with optimal 42 degrees tilt, corresponding to 12.2 kW_p.

storages such as for example batteries were concluded in [28] to be the most effective option for increasing self-consumption, at least for a higher penetration level. The increasing amount of EVs in the world has led to higher interest for EV battery as potential PV power storage [30]. For a recent review of PV power self-consumption, see [37].

2.3.4 Modeling photovoltaic power production

The first statistical investigations of the relation between sunshine and cloudiness were carried out by Ångström nearly a century ago [38, 39, 40]. Early investigations indicated that the relative amount of sunshine compared with clear-sky conditions — called the clear-sky index — was bimodally distributed or at least that it displayed asymmetry with respect to the mean value [41, 42, 43, 44, 45, 46]. These studies were followed by characterizations of daily and hourly probability distributions [47, 48, 49, 50]. Over time the resolution improved from 5-minute to 1-minute to near instantaneous [51, 52, 53, 54]. A complete model of instantaneous radiation is yet to be achieved [55].

Examples of distribution families include single Gamma distribution [49], single Boltzmann distribution [48], Bi-exponential [56], double Normal distributions [53], double Beta distributions [57], double Boltzmann distributions [54], Logistic combined with Weibull [58] and triple Normal distributions [55]. There appears no preference in the literature for a particular distribution family for representing the clear-sky index. Modeling the clear-sky index for various conditions and locations is directly useful for estimating the PV power production variability and overall potential.

2.4 Household electricity use

The total electricity use in Sweden 2012 was 128 TWh whereas 21 TWh represented household electricity use [59]. Thus, quantifying household electricity use patterns and variability can contribute significantly to the understanding and predictions regarding Swedish energy use over time. Quantifying household electricity use is also valuable for integrating distributed renewable energy supply in the built environment and designing electricity distribution grids for urban or rural communities [8, 60, 61]. However, household electricity use with high time resolution is complex to quantify. Not only are there seasonal and diurnal variations in electricity use from for example heating and lighting, but the load is also highly stochastic [62]. The complexity of describing human activities over time suggests an interdisciplinary approach where both quantitative and qualitative research is useful in order to properly characterize domestic electricity use [61].

2.4.1 Modeling household electricity use

Based on monitoring data from households it is possible to study electricity use via devising "bottom-up" models based on assumptions or data for activity patterns, appliance use and appliances [61, 63, 64, 65, 66, 67, 68, 69, 70]. Here [63, 65, 66, 69, 70] make use of detailed information on household appliances and occupancy to model electricity use of any number of households while [9, 10, 67, 68] use data on occupancy and appliances to construct stochastic models. Here bottom-up modeling means estimating household electricity use based on activity patterns or individual household electricity data with the aid of some assumptions as a means for estimating electricity use for individual households and then potentially estimating this for a regional or national scenario [60, 62].

Conversely a "top-down" approach only typically considers the residential sector as an energy sink with no resolution of individual households [60, 62]. Top-down models need only aggregate data while bottom-up models need more detailed data on household level [60].

The problem of quantifying individual household electricity use by means of bottom-up strategies could be condensed to quantifying three factors: (a) the set of appliances in the household, (b) the electricity use of the appliances and (c) the appliance use patterns [9]. The stochastic nature of household electricity use mostly stems from (c), which is mainly the result of human activities.

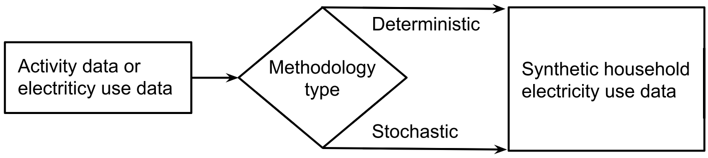

Figure 2.5. Deterministic and stochastic bottom-up models of household electricity use based on activity data or electricity use data.

Activity patterns can be used to estimate electricity use in households. There are many approaches to characterizing and quantifying household activity patterns [71]. One of these approaches is the method involving *time-use data* (TUD), in particular via so-called *time diaries*. This concept involves collecting data about the particular states of activity for residents in households [71]. These time diaries are distributed to residents with the intent that they write down their activities over time [71, 72]. One assumption in the time diary approach is that each resident only occupies one state at the time, and that they at any time may switch from one state of activity to another [9, 10, 73]. Time-use data was used as the basis for the Widén Markov chain model for household electricity use described in Section 3.3.1.

As an example of electricity use data there is a data set provided by the Swedish Energy Agency, which was thoroughly analyzed in [74], and used in papers (III), (VIII) for developing probability distribution models. See Section 3.3.2 for more information.

For bottom-up modeling based on time-use data or electricity use data on the household level there are two methodologies: deterministic and stochastic modeling. A deterministic model is defined as always producing the same output given the same input. In contrast a stochastic model is calibrated with input data and produces synthetic output which not necessarily gives the same output for the same input [75]. A deterministic model can for example be used to give a direct connection between activity data and electricity consumption. A stochastic model is used to produce synthetic activity patterns which can then for example be used in power system calculations. Both deterministic and stochastic models of energy use may be based on time use data, see Figure 2.5.

Examples of deterministic approaches for estimating household energy use are [63, 64]. Stochastic approaches to modeling household electricity use include Markov chain modeling [9, 10, 67, 68] and probability distribution modeling [69, 76, 77, 78, 79, 80, 81, 82]. It is also possible to characterize household electricity use by other means, such as for example by using clustering [83]. A conclusion which can be drawn from the literature is that there is generally no unique or canonical distribution type suitable for modeling household electricity use [76, 84]. However there are benefits associated with probability distribution modeling such as the possibility to use analytic calculations regarding grid interaction [7].

2.5 Electric vehicles

The first EV was built by Gustave Trouvé from France in 1881 [85, p.12]. It was a tricycle powered by a 0.1 horsepower electric motor fed by lead-acid batteries. As gasoline powered vehicles started to become more powerful, flexible and easier to handle the EV started to disappear from the market [85]. The efficiency related to power regulation of the EV was improved in the 1940's with the invention of the transistor. The most prominent EVs that used this updated technology was perhaps the Lunar Roving Vehicle, which the Apollo astronauts used on the Moon [86]. Despite advances in battery technology and power electronics in the 1960's and 1970's the EV range was still a significant obstacle [85]. During the 1980's a number of EVs from major car manufacturers were released, for example the EV1 from GM. Throughout EV history the main problem has been battery capacity, and above all the amount of energy it can store per kilogram weight.

Today EVs have diversified into several sub-types of electric and hybrid electric vehicles which have different niches and applications.

2.5.1 Modern electric and hybrid electric vehicles

Despite having a long history EV technology was revived in a large-scale global development program in the 1990s [87]. Today the electric vehicle concept covers a wide range of different types of vehicles. Plug-in electric vehicles (PEVs) have an electric motor and the possibility to be charged from the grid. The performance sedan Tesla model S [88] (see Figure 2.6), the two-seat Renault Twizy [89] and the best-selling electric vehicle in the world Nissan Leaf [90] are examples of modern PEVs [91].

There are also hybrid electric vehicles (HEVs) which have both an electric engine and an internal combustion engine (ICE). The best selling HEV is the Toyota Prius [92]. There are also plug-in hybrid electric vehicles (PHEV), for example limited production supercars such as McLaren P1 [93], Porche 918 [94] and Ferrari LaFerrari [95] but also standard production cars such as the top selling PHEV Chevrolet Volt [91]. Additionally, there exist experimental and concept EVs with on-board PV modules for charging the battery, an examples of this type of vehicle is the concept car NLV Quant [96]. These main types of electric vehicles cover electric vehicles that in scale and function aim to mimic ordinary vehicles with ICEs. There are other types of vehicles with electric propulsion such as the two-wheeled self-balancing Segway PT [97] and electric bicycles (e-bikes). The EVs which are considered in this thesis are mainly PEVs and PHEVs.

Figure 2.6. A Tesla model S in a Tesla retail store. Photo: Joakim Munkhammar 2014.

About 604,000 PEVs, PHEVs and electric utility vans were sold worldwide by September 2014 [91], whereas 247,700 were plug-in hybrids. USA has the largest amount of EVs [98] in the world but Norway had the largest percentage of EVs in terms of market share in 2013 [99]. The Swedish car fleet had about 4.5 million cars registered for use in 2013 [100], out of those 1,010 were pure EVs. But a total of about 28,000 were HEVs and out of those 1,671 PHEVs [100].

2.5.2 Electric vehicle engine and battery

The electric motor has an efficiency of about 80 percent which can be compared with the around 30 percent efficiency of ICEs [101]. While ICEs typically run on gasoline, diesel or biofuel the electric engine is usually powered by a battery. Since an EV is typically powered from the grid the stored battery energy has its origin in the current energy mix. Apart from the cost one important aspect of a battery is its ability to contain stored energy per kilogram — the so-called specific energy of the battery [102]. There are many types of rechargeable batteries such as for example lead-acid, nickel-cadmium, nickel-metal hybride, lithium-ion and lithium-polymer. With high specific power, cycle lifetime and an energy density of about 150 Wh/kg [103] lithium-ion batteries are particularly useful, and is the most common type of battery used in modern EVs [104]. The lifetime and performance of modern batteries is reduced with deep discharges and affected by external temperatures [105]. The battery on board EVs are currently expensive and have low specific energy compared to fuel for ordinary ICEs [104, 105]. As an example of battery capacity for different types of EVs Renault Twizy has 6.1 kWh [89], Nissan Leaf has 24 kWh [90], and Tesla Model S has 60-85kWh depending on version [88].

2.5.3 Electric vehicle grid interaction

When a PEV or PHEV is plugged into the grid there are several possibilities for charging worldwide without any universal standard at the current time. In Sweden the most common type of connection available is the one phase outlet which allows for charging of 2.3 kW (230V, 10A) AC. It is also possible to fast charge EVs with for example CHAdeMO [106, 107] charging type with maximum charging power of 50 kW [108]. There is also the Tesla supercharger, distributed across US, Europe and Asia, which can deliver 90 kW charging [109].

The most common type of charging is conductive technology, but inductive solutions are also being considered [110]. Another possibility is to have replaceable batteries and battery swapping stations [111].

In contrast to using the EV battery only as a storage, meaning power flow only in one direction, it is in practice possible to reverse the power flow and enable the EV to deliver power to the grid [112, 113]. A collective name for these technologies is Vehicle to Grid (V2G) [112]. The work presented in this thesis does not include any simulations of V2G.

2.5.4 Modeling electric vehicle charging

EV charging and grid interaction has been studied considerably recently [114, 115, 116, 117]. Studies regarding smart charging have been presented [118, 119] and more efficient battery management systems have been investigated [120, 121, 122]. Generally the feasibility of model approaches and renewable energy use in EV grid integration [123] and strategies for energy management for plug-in hybrid EVs have also been studied [122, 124]. Regional studies on the grid-impact of EV charging have been made, such as for Swedish conditions [125, 126].

The possibility of on-board PV power production has been investigated [127]. Recent studies also investigate the benefit of using PV as a curtailment of PHEV load on a large scale [36, 128, 129], and there are case studies regarding co-benefits of EV charging and PV power production [130]. In general there seems to be a consensus in the literature that the introduction of EVs in the grid has a potential to assist renewable energy integration into the grid [123, 127, 128, 131], albeit with the potential for new problematic issues [131]. A common theme is also that smart charging, which a collective name for charging strategies and advanced charging technologies, is necessary in order to properly introduce EVs into the grid [123]. However, in order to devise smart-charging strategies a first step is to quantify the interaction with other sources and sinks of electricity such as household electricity use, PV power production and uncontrolled EV charging.

As regards EV charging there exist many studies that investigate uncontrolled EV charging based on user habits, e.g. [132, 133, 134, 135, 136, 137, 138, 139, 140, 141, 142, 143, 144]. EV charging can be modeled using predefined time periods for charging [137, 141] and charging only after all trips of the day made with the vehicle [134, 135, 138, 140]. Also general spatial and temporal charging has been investigated recently [145]. Models for EV charging can be deterministic [135, 136], stochastic with the use of Monte Carlo simulations [134], Markov chains [138, 146] or distributions [140, 144, 147, 148, 149].

2.6 Identified research gaps

The existing scientific literature includes large amounts of research on PV power production, household electricity use, EV charging and combinations thereof. This section lists and summarizes identified research gaps, and how the research in this thesis assist in filling them.

- *Photovoltaic power production*. The current state-of-the-art science of solar irradiance is in need of further studies, in particular regarding variability over space and time as well as applicability in fields such as PV power production. Paper (I) develops a model for PV power production which is useful for computing PV power production on arbitrarily oriented surfaces and for dispersed locations. Paper (II) introduces a new approach to modeling solar irradiance by convolution of probability distributions as a means to characterize variability of solar irradiance.

- *Household electricity use*. For load matching with for example PV power production as well as for the design and operation of local electricity grids there is a need to characterize individual and aggregate household electricity use, in particular based on high resolution regional data. Paper (III) develops a probability distribution model using a large data set on recent household electricity use in Sweden, which is used directly to characterize aggregate household electricity use.

- *Electric vehicle charging*. The lack of EV charging data, and the necessity for quantifying EV charging, has generated a vast amount of EV charging models in the literature. It can be concluded that there is a particular interest for applicable models and models which are based on regional data, which can be used for regional studies. In papers (IV) and (V) stochastic models for different types of EV charging were developed based on Swedish driving habits. In paper (IX) we present and analyze meter data on EV charging.

- *Grid interaction.* In terms of grid interaction most studies have focused on the separate components of PV power production, household electricity use and EV charging. There is a shortage of stochastic models combining all components, while for design and operation of the electricity grid there is a need to quantify this variability. In particular no probability distribution model combining all components exist in the literature. Paper (VII) aims to provide a combination model based on the data for PV power production, the Widén Markov chain model for household electricity use and the EV home-charging model developed in paper (IV) based on the Widén model. In paper (VI) this setup is applied to a case study for the City of Westminster, London. Finally in paper (VIII) a state-of-the-art probability distribution model for the interaction of electricity consumption and production from the complete system is developed.

3. Methodology and data

In this chapter the methodology and data used in this thesis is presented. In Section 3.1 the mathematical methodology is presented. In Section 3.2 PV power production models and data are outlined, followed by model descriptions of household electricity use in Section 3.3 and EV charging models and data in Section 3.4. Data from the solar charging stations is presented in Section 3.5. Finally self-consumption methods and measures are presented in Section 3.6.

3.1 Mathematical modeling

The work presented in this thesis is to a large extent based on mathematical modeling by means of using different mathematical and statistical methods. In this section these general methods are presented. It should be noted that most model simulations and data analysis in this thesis were carried out with MATLAB, when nothing else is mentioned.

3.1.1 Markov chain modeling

A discrete-time Markov chain $\mathbf{S}_t$ is a discrete stochastic process which occupies one state E_μ out of a number of states in a state-space $\mu \in [1,...,N]$ for each time step t. For the application in this thesis N is the number of states and T is the number of time-steps. The probability for each state to become occupied in the next time-step is calculated on the basis of the transition matrix $Q_{\mu\nu}(t)$ defined for the stochastic variable X_t at time-step t [75]:

$$Q_{\mu\nu}(t) = \text{Prob}(X_{t+1} = E_\nu | X_t = E_\mu). \tag{3.1}$$

The transition matrix for a particular model can be estimated from a time series of states. Markov chains are used in papers (IV), (VI) and (VII). A schematic illustration of a Markov chain process is given in Figure 3.1.

3.1.2 Probability distribution modeling

Probability distribution modeling in this thesis consists of calibrating probability density functions (PDFs) based on data, and in turn utilizing statistical properties of these distributions as tools for modeling. In this thesis Normal,

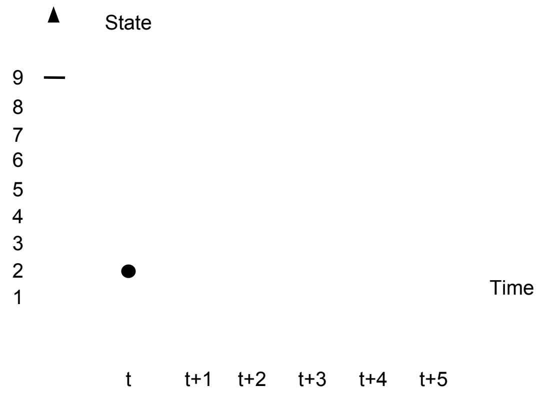

Figure 3.1. A schematic illustration of a Markov chain process entering one state at a time.

Log-normal, Weibull, Gamma and Bernoulli distributions are used, and are presented below. For a more thorough mathematical account of these distributions see [150]. Probability distributions were used in papers (I), (II), (III), (V) and (VIII).

The *Normal*, or *Gaussian*, PDF is defined as (see, for instance, [150]):

$$f_N(x;\mu,\sigma) = \frac{1}{\sigma\sqrt{2\pi}} e^{-\frac{(x-\mu)^2}{2\sigma^2}}, \quad -\infty < x < \infty, \tag{3.2}$$

with mean value μ and variance σ^2. When integrating (3.2) one arrives at the Normal cumulative distribution function (CDF):

$$F_N(x;\mu,\sigma) = \frac{1}{2}\left[1 + \mathrm{erf}\left(\frac{x-\mu}{\sigma\sqrt{2}}\right)\right], \tag{3.3}$$

where $\mathrm{erf}(x)$ is the error-function defined by [152, p.297]:

$$\mathrm{erf}(x) = \frac{2}{\sqrt{\pi}} \int_0^x \mathrm{e}^{-t^2} \mathrm{d}t. \tag{3.4}$$

There is also have the PDF of a *Log-normal* distributed stochastic variable [150]:

$$f_L(x;\mu,\sigma) = \frac{1}{x\sigma\sqrt{2\pi}} \mathrm{e}^{-\frac{(\ln x-\mu)^2}{2\sigma^2}}, \quad x > 0, \tag{3.5}$$

where $\exp(\mu + \sigma^2/2)$ is the mean value and $(\exp(\sigma^2) - 1) \times \exp(2\mu + \sigma^2)$ is the variance. The integrated version of (3.5), the CDF of a Log-normal variable, is:

$$F_L(x;\mu,\sigma) = \frac{1}{2}\left[1 + \mathrm{erf}\left(\frac{\ln(x)-\mu}{\sigma\sqrt{2}}\right)\right]. \tag{3.6}$$

The PDF of a *Weibull* distributed random variable is defined by (see eg. [150, p.61], [151]):

$$f_W(x;\lambda,k) = \begin{cases} \frac{k}{\lambda}\left(\frac{x}{\lambda}\right)^{k-1}\mathrm{e}^{-(x/\lambda)^k} & x \geq 0, \\ 0 & x < 0, \end{cases} \tag{3.7}$$

where $k > 0$ is the *shape parameter* and $\lambda > 0$ is the *scale parameter*. The integrated version of (3.7), the cumulative distribution function (CDF) of a Weibull distributed random variable, is:

$$F_W(x;\lambda,k) = \begin{cases} 1 - \mathrm{e}^{-(x/\lambda)^k} & x \geq 0, \\ 0 & x < 0. \end{cases} \tag{3.8}$$

For the special case of $k = 1$ the Weibull distribution is equivalent to the exponential distribution and for $k = 2$ it is equivalent to the *Rayleigh* distribution. The distribution has the following mean value (μ):

$$\mu = \lambda\Gamma(1 + 1/k), \tag{3.9}$$

and the variance (σ^2):

$$\sigma^2 = \lambda^2[\Gamma(1+2/k) - (\Gamma(1+1/k))^2] \tag{3.10}$$

Here $\Gamma(x)$ is the Γ-function which can be defined through the Euler integral [152, p.255]:

$$\Gamma(x) = \int_0^\infty t^{x-1}e^{-t}dt, \tag{3.11}$$

for which $\Gamma(n) = (n-1)!$ holds for any positive integer n. There is also the *Gamma* distribution, which has the following PDF [150, p.60]:

$$f_G(x;k,\delta) = \frac{1}{\delta^k\Gamma(k)}x^{k-1}e^{-x/\delta}, \quad for \quad x,k,\delta > 0. \tag{3.12}$$

The Gamma distribution has mean value $k\delta$ and variance $k\delta^2$. The integrated version of (3.12) gives the Gamma CDF:

$$F_G(x;k,\delta) = \frac{\gamma(k,x/\delta)}{\Gamma(k)}, \tag{3.13}$$

where $\Gamma(k)$ is the Gamma function, see (3.11) and $\gamma(k,\theta)$ is the (lower) incomplete Gamma-function:

$$\gamma(k,\theta) = \int_0^\theta t^{k-1}e^{-t}dt. \tag{3.14}$$

The probability mass function (PMF) f_B of a *Bernoulli* distributed stochastic variable is defined as:

$$f_B(k,p) = \begin{cases} p & \text{if } k = 1, \\ 1-p & \text{if } k = 0, \end{cases} \tag{3.15}$$

with mean value p and variance $p(1-p)$. The Bernoulli PMF can also be written in terms of the Binomial PMF:

$$f_B(k,p) = p^k(1-p)^{1-k} \sim \text{Bernoulli}(p) \sim \text{Bin}(1,p), \quad for \quad k \in [0,1], \tag{3.16}$$

where the Binomial PMF is defined as (see for instance, [150]):

$$\begin{aligned} f_{bin}(k,n,p) &= \binom{n}{k} p^k(1-p)^{n-k} \qquad (3.17) \\ &= \frac{n!}{k!(n-k)!} p^k(1-p)^{n-k}, \quad k = 0,\ldots,n. \end{aligned}$$

The CDF of the Bernoulli distribution is defined by:

$$F_B(k,p) = \begin{cases} 0 & \text{if } k < 0, \\ 1-p & \text{if } 0 \leq k < 1, \\ 1 & \text{if } k = 1. \end{cases} \tag{3.18}$$

3.1.3 Convolution and the central limit theorem

In application it can prove useful to define the sum of stochastic variables $X_1, X_2, ..., X_N$:

$$S_N = \sum_{i=1}^{N} X_i. \tag{3.19}$$

Finding an explicit mathematical expression for the distribution of S_N means finding the convolution of the probability distributions for each stochastic variable. Obtaining an analytic expression for the convolution of any set of distributions can be difficult, and sometimes it is not even even possible. This difficulty is present even if the stochastic variables are independent. In this thesis convolutions of Normal, Log-normal, Weibull and Bernoulli distributions as independent variables are investigated in papers (I), (III) and (V). Also a convolution involving dependent variables is investigated in paper (VIII). The convolution of N stochastic variables from each distribution family considered in this thesis is shown in Table 3.1.

As shown in Table 3.1 there are no analytic expressions for the convolution of the Weibull and Log-normal distribution families. However it should be emphasized that there exist analytic convolution expressions for the N-fold convolution of approximate distributions [153, 154].

Even though it might not be possible to obtain analytic expressions for the convolution of N PDFs it is possible with the *central limit theorem* to give limiting distributions for large N [150, p.91]. This theorem states that for N independent stochastic variables $X_1, X_2, ..., X_N$ from the same distribution f with expected value $E[X] = \mu$ and variance $V[X] = \sigma^2$ the mean of the

Table 3.1. *Distributions and convoluted distributions.*

Distribution family	N-variable convolution	Parameter range
Normal(μ,σ)	Normal$\left(\sum_{n=1}^{N}\mu_i, \sum_{n=1}^{N}\sigma_i^2\right)$	$-\infty < \mu_i < \infty$, $\sigma_i^2 > 0$
Bernoulli(p)	Binomial(N,p)	$0 < p < 1, N = 1,2,...$
Gamma(α,β)	Gamma$\left(\sum_{i=1}^{N}\alpha_i, \beta\right)$,	$\alpha_i > 0$, $\beta > 0$
Log-normal(μ,σ)	$---$	$---$
Weibull(k,λ)	$---$	$---$

variables as N grows large is normally distributed with expected value $E[X] = \mu$ and variance $V[X] = \sigma^2/N$:

$$f_N(x,\mu,\sigma/\sqrt{N}) = \frac{\sqrt{N}}{\sigma\sqrt{2\pi}}\mathrm{e}^{-\frac{(x-\mu)^2 N}{2\sigma^2}}. \tag{3.20}$$

This theorem allows for an approximate analytic expression for the PDF of large numbers of independent stochastic variables. This theorem was used in papers (I), (III) and (V).

3.1.4 Mixture distributions

A mixture distribution $f(x)$ over the variable x is defined as the sum of a number of PDFs $f_i(x)$ with weights w_i:

$$f(x) = w_1 f_1(x) + w_2 f_2(x) + ..., \tag{3.21}$$

where $f_i(x)$ typically belongs to some family of distributions such as for example Normal, Log-normal or Weibull. Two important aspects arise in statistical modeling with mixture distributions: on the one hand, the number of mixtures, on the other, the family of probability distributions (the same family of distribution is here assumed for all components of the mixture). However, care has to be taken regarding the number of modes (which are equivalent to local maxima in the probability density function) versus the number of actual populations. For instance, it can be shown that for the mixture of two normally distributed populations, the mixture probability density is bimodal if and only if $|\mu_1 - \mu_2|/\sigma > 2$, where (μ_1, μ_2) are the two means and σ^2 is the common variance [155]. A mixture of one distribution is called a unimodal distribution, a mixture of two distributions is called a bimodal distribution and a mixture of three distributions is called a trimodal distribution. Mixture distributions were used in paper (I) and indirectly in paper (VIII).

3.1.5 Parameter estimation

In this thesis the estimation of parameters for the distributions was made with a maximum likelihood estimation [156]. In such an estimation, given data set values $x = \{x_1, x_2, ..., x_N\}$ and an assumed PDF f with unknown parameters μ, σ, the likelihood function:

$$L_f(x;\mu,\sigma) = f(x_1;\mu,\sigma) \times f(x_2;\mu,\sigma) \times ... \times f(x_N;\mu,\sigma) = \prod_{i=1}^{N} f(x_i;\mu,\sigma) \tag{3.22}$$

is maximized in order to obtain the parameters μ and σ, see [150, p.80] for more information. An illustration of a histogram from fictive data and a fictive PDF fit to the data is given in Figure 3.2.

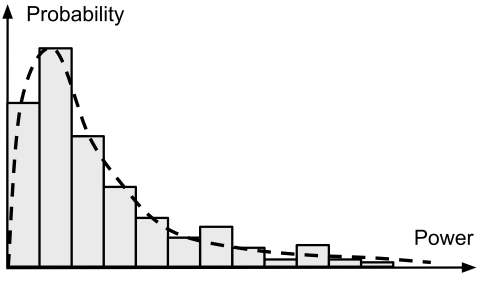

Figure 3.2. An illustration of fictive data in a histogram along with a fictive distribution which is fit to the data.

3.1.6 Kolmogorov-Smirnov test

To estimate the goodness of fit between original data sets and proposed distributions, several tests exist in the literature. A commonly used test is the two-sample Kolmogorov–Smirnov (K-S) test. This test is based on the maximum deviance between two distribution functions, and tables with critical values (or their implementations in statistical software) can be used to deduce statistical significance. A test quantity D can be formulated as:

$$D = \max_x |F_1(x) - F_2(x)| \tag{3.23}$$

where $F_1(x)$ and $F_2(x)$ are cumulative distribution functions. It is possible to compare distribution families or data using this method. K-S tests were used in papers (I), (III) and (VIII), where data was generated from each distribution and compared with original data. The smaller D is the better fit the distribution is. It should be noted that although more specialized tests have been developed for e.g. the Weibull distribution, the Kolmogorov–Smirnov test remains widely used [151, 157].

3.2 Photovoltaic power production

This section will present models and data used in the appended papers regarding:

- Solar irradiance.
- Conversion of solar irradiance from the horizontal plane to the tilted plane.
- PV power production.

In papers (I), (II) and (VIII) models of solar irradiance were developed and applied, and in papers (I), (II), (VI) and (VIII) conversion of solar irradiance from the horizontal plane to tilted plane was used in applications to PV power production. In paper (IX) data on PV power production was analyzed.

3.2.1 The clear-sky index

The variability of solar irradiance at any location is dependent on two things: the deterministic path of the sun across the sky and the stochastic variability of atmospheric conditions. The solar irradiance on a horizontal surface is defined by the Global Horizontal Irradiance (GHI). GHI can in turn be decomposed into Diffuse Horizontal Irradiance (DHI) and Beam Horizontal Irradiance (BHI) according to:

$$G = G_b + G_d, \tag{3.24}$$

where G =GHI, G_b =BHI and G_d = DHI. This can be normalized by the GHI for clear-sky G_c, which is defined as the so-called clear-sky index κ:

$$\kappa \equiv \frac{G}{G_c} = \kappa_b + \kappa_d. \tag{3.25}$$

Here G_c is the GHI for clear-sky, which is determined by the sun's position on the sky dome. The clear-sky index represents the stochastic part of solar irradiance on a horizontal surface since it suffices to multiply the clear-sky index by G_c to obtain solar irradiance.

3.2.2 Bimodal probability distribution model

As a means to model solar irradiance a probability distribution model was developed in paper (I). This model was based on the clear-sky index, which in turn was used used to model solar irradiance and PV power production, see Sections 3.2.5 and 3.2.6 for the latter part. The main idea was to fit a PDF to the clear-sky index data set, which is shown in the histogram in Figure 3.3.

The data for solar irradiance that was used to estimate the clear-sky index was one-minute resolution over one year (2008) obtained from SMHI for Norrköping, Sweden (59°35′31” N 17°11′8” E) [158]. Global clear-sky irradiance was calculated with the Ineichen-Perez model [159]. In order to avoid infinities associated with low solar angles the clear-sky index was only obtained for solar angles above 20 degrees. The total number of one-minute resolution data points used was then 111,221.

It should be noted that estimating the clear-sky index from data requires the process of estimating global horizontal clear-sky irradiance for each time-step. This includes for example the sun's position on the sky dome, but also assumptions regarding atmospheric turbidity. Since this can underestimate and overestimate the clear-sky index in the order of a few percent, this setup serves as an approximation. The mean of the clear-sky index, and the position of the peaks of the distribution, are then likely scaled by a few percent.

This model consists of a fit-to-distribution approach of the clear-sky index to a bimodal distribution, which is a common approach in the solar irradiance research community, see e.g. [41, 42, 43, 44, 45, 46]. A bimodal distribution is a two-distribution special case of mixture distributions, see Section 3.1.4.

It is possible, by visual inspection, to observe two or three peaks in the histogram of the clear-sky index in Figure 3.3.

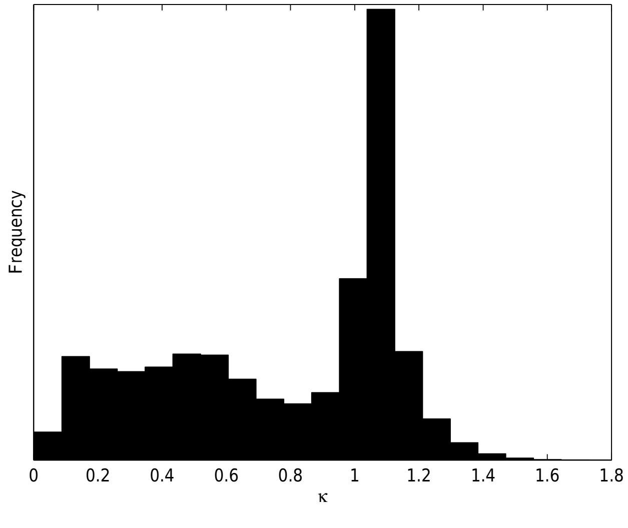

Figure 3.3. A histogram over the clear-sky index from the one-year minute resolution data set obtained for Norrköping, Sweden, during 2008 [158].

A standard tool for estimation of mixture models is the EM (Expectation–Maximization) algorithm, see Section 3.1.5. A version implemented in the software R and found in the package mixtools was used [160]. Parameters for the distributions and mixing weights were obtained. The goodness-of-fit

Table 3.2. *Estimated parameter values for the bimodal Normal distribution of clear-sky index using* (3.26).

μ_1	μ_2	σ_1	σ_2	w_1	w_2
0.58	1.07	0.35	0.04	0.63	0.37

for this model was estimated with the use of Kolmogorov-Smirnov tests, see Section 3.1.6 for more information on that.

In paper (I) mixture distributions with unimodal, bimodal and trimodal Normal distributions were investigated. A bimodal Normal distribution was chosen since it was best fit according to K-S tests. According to the setup of mixture distributions in Section 3.1.4 a bimodal Normal distribution $f(x)$ with variable x can be written as:

$$f(x) = w_1 f_N(x;\mu_1,\sigma_1) + w_2 f_N(x;\mu_2,\sigma_2) \tag{3.26}$$

where w_1 and w_2 are weights, μ_1 and μ_2 are the mean values, σ_1 and σ_2 are the variance for each Normal distribution in this bimodal configuration. Assuming that the clear-sky index can be modeled as a bimodal Normal distributed stochastic variable with estimated parameters in Table 3.2, then (3.26) represents an approximate probability distribution of the clear-sky index.

3.2.3 Solar irradiance for remote locations

The bimodal probability distribution model of the clear-sky index was designed for modeling probability distributions for solar irradiance with the intent of estimating PV power production for a single location. By defining the clear-sky index as a stochastic variable it was also possible to model the aggregate solar irradiance for multiple remote (uncorrelated) locations. As an extension to the clear-sky index an aggregate clear-sky index was defined for any number of dispersed uncorrelated locations.

In similarity with the single-location clear-sky index κ the aggregate clear-sky index, here denoted by $\bar{\kappa}_N$ for N locations, was assumed to be a stochastic variable defined as the average of N stochastic variables:

$$\bar{\kappa}_N = \frac{1}{N}\sum_{i=1}^{N} \kappa_i, \tag{3.27}$$

where κ_i represents the clear-sky index at each remote location i. See [49, 55, 161, 162, 163, 164] regarding the decline of correlation with distance for pairs of locations. Results regarding aggregate clear-sky index will be analyzed in Section 4.1.1.

3.2.4 Convolution approach

As an alternative approach to modeling solar irradiance via probability density distributions a convolution approach was introduced in paper (II).

By treating BHI and DHI as stochastic variables it was conjectured in paper (II) that GHI could be obtained via a convolution of probability distributions for BHI and DHI. Since there is a complex dependency between BHI and DHI, the study in paper (II) was setup as an initial study with the aim to provide estimates mainly regarding expected values. This proved useful for the derivation of a generalized form of the Ångström equation, which had empirically been conjectured by Anders Ångström in 1922 [38, 39, 40]. The methodology for this ansatz is described below and the derivation of the generalized Ångström equation is presented as a main result of that study in Section 4.1.2.

The clear-sky index can be decomposed into the diffuse and beam components according to $\kappa = \kappa_d + \kappa_b$ as was described in Section 3.2.1. It should be emphasized here that there is a complex dependency between κ_d and κ_b[165]. Modeling such a dependency requires a detailed statistical analysis, which is outside the scope of paper (II), which aims to show that such an approach has a deep connection to a generalized Ångström equation. A complete model including the dependency of κ_b and κ_d is yet to be achieved.

If κ_d is assumed to be represented by a stochastic variable X_d and κ_b is represented by a stochastic variable X_b, then an analogue for κ can be defined as stochastic variable X:

$$X = X_d + X_b, \tag{3.28}$$

which constitutes a convolution of the probability distributions for the stochastic variables X_d and X_b (see Section 3.1.3 on convolutions of probability distributions). In the literature the distribution for empirical measurements of κ_d is typically assumed to be unimodal whereas κ_b is assumed bimodal [54]. As an approximation it is here assumed that the bimodal peaks of κ_b correspond to two states: bright sunshine, no bright sunshine [165]. This is motivated by the fact that beam irradiance essentially only reaches the Earth's surface when no clouds obscure the sun [165]. That is, κ_b is approximately a two-state distribution with one peak close to zero corresponding to cloud coverage blocking the sun and one peak between zero and one corresponding to bright sunshine. The bright sunshine peak is dependent on the interpretation of the definition "bright sunshine" in this particular probability distribution approach. A scaling parameter β is introduced that relates the beam irradiance distribution X_b to a two-state Bernoulli distribution (See Section 3.1.2):

$$X_b = \beta X_b', \tag{3.29}$$

where:

$$X_b' \sim \text{Bernoulli}(p). \tag{3.30}$$

The scaling factor β is assumed to be the average beam irradiance index above a threshold σ. This also defines p as the proportion of beam irradiance index fractions greater than σ. In total this represents a fit-to-distribution for the beam irradiance index by means of a weighted Bernoulli distribution. Any calibrated unimodal distribution valid for $x \geq 0$ such as Gamma, Weibull or Log-normal PDFs could be used to model the diffuse stochastic variable X_d in this particular study. As a typical positive unimodal PDF the Gamma PDF was by inspection chosen to represent the diffuse stochastic variable: $X_d \sim \text{Gamma}(\sigma, \delta)$. For detailed information on the distributions, see Section 3.1.2.

In this study the parameters γ and δ were set by the fit-to-distribution routine *gamfit* in MATLAB. The data set used in the simulations in paper (II) was a one-year minute-resolution data set on DHI and BHI for the location of Norrköping, Sweden (59°35′31” N 17°11′8” E) from 2008 [158]. Global clear sky irradiance was calculated with the Ineichen-Perez model [159]. In order to avoid infinities in the data set the clearness indices were only evaluated for solar angles above 20 degrees. This constitutes the convolution model for solar irradiance in paper (II). Results and the derivation of the generalized Ångström equation are given in Section 4.1.2.

3.2.5 Conversion of solar irradiance from the horizontal to the tilted plane

With measured or synthetic data on solar irradiance it is useful for modeling PV power production to be able to calculate solar irradiance on a tilted plane. In order to do this a number of transformations are required, which can be performed in this order:

1. Split GHI into DHI and BHI.
2. Convert DHI and BHI to the tilted plane of the PV array.
3. Apply models for the PV system components, e.g. PV modules and inverter.

There are many options available for all three steps. The following is one option, and it was used in papers (I) and (VIII).

In order to simulate a PV system with arbitrary orientation, in terms of tilt angle β and azimuth angle γ, GHI has to be split into BHI and DHI because these components have different incident angles on the tilted plane and thus need to be re-scaled separately. Several models have been proposed to determine the diffuse fraction of GHI, for a review of models see [166]. The Erbs model [167] was used in paper (I), and indirectly in paper (VIII).

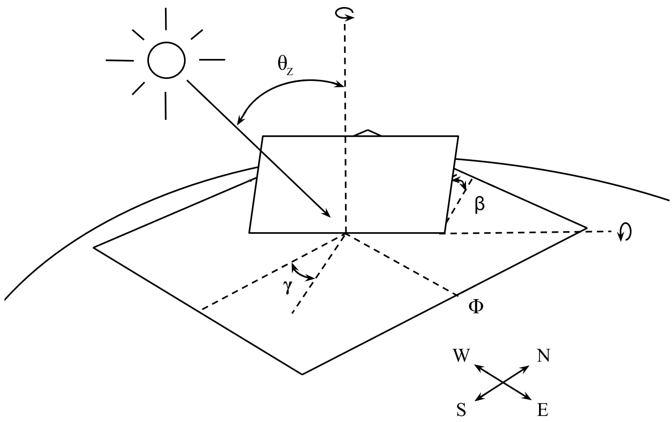

Figure 3.4. A schematic illustration of angles associated with a tilted plane relative to the horizontal plane. β is tilt, γ is azimuth and θ_z is the zenith angle of incidence.

The diffuse fraction κ_d is

$$\kappa_d = 1 - 0.09\kappa \text{ for } \kappa \leq 0.22,$$
$$\kappa_d = 0.9511 - 0.1604\kappa + 4.388\kappa^2 - 16.638\kappa^3 + 12.336\kappa^4 \text{ for } 0.22 < \kappa \leq 0.80,$$
$$\kappa_d = 0.165 \text{ for } \kappa > 0.80. \tag{3.31}$$

The diffuse and beam radiation components from (3.24) are then obtained by:

$$G_d = \kappa_d G, \tag{3.32}$$

$$G_b = (1 - \kappa_d)G. \tag{3.33}$$

Next, radiation on the tilted plane is obtained by scaling beam radiation by the geometric factor $R_b = \cos\theta / \cos\theta_z$, where θ and θ_z are the incidence angles for beam radiation on the tilted plane and the horizontal plane, respectively [168], see illustration in Figure 3.4. Diffuse and ground-reflected radiation on the tilted plane have to be calculated with other, semi-empirical models. With the Hay & Davies model for diffuse radiation, which was also used in paper (I), the global radiation on the tilted plane is given as [168]:

$$G_T = G_b R_b + G_d \left[(1 - A_i) \left(\frac{1 + \cos\beta}{2} \right) + A_i R_b \right] + G\rho_g \left(\frac{1 - \cos\beta}{2} \right) \tag{3.34}$$

where the anisotropy index A_i is the ratio between the incident beam radiation G_b and the extraterrestrial radiation G_0 on the horizontal plane, β is the tilt angle of the plane and ρ_g is the ground reflectance. This can then be connected to models of PV power production.

3.2.6 Photovoltaic system simulations

With available measured or synthetically generated data on solar irradiance on tilted surfaces it is possible to model PV power production for any arbitrarily oriented PV system.

For irradiance G_T a simple model for the DC output from the PV array is:

$$P_{dc} = AG_T\eta_m(1-q_a) \tag{3.35}$$

where A is the area of the array, η_m is the PV module efficiency and q_a accounts for different losses in the PV array not modeled explicitly.

The inverter in the PV system limits the output AC power to its rated power, and is therefore important to include in the model since there is a finite probability, albeit small, that very high κ samples are obtained, leading to high DC powers being cut by the inverter. The output AC power can be modeled as [169]:

$$P_{ac} = P_{ac0}\frac{P_{dc}-P_{s0}}{P_{dc0}-P_{s0}} \tag{3.36}$$

for P_{dc} values between P_{s0} and P_{dc0} where P_{ac0} is the rated inverter AC power, P_{dc0} is the DC power at which the AC rating is achieved and P_{s0} is the inverter threshold power, i.e. the lowest DC input that gives an AC output. Below P_{s0} the output is zero and above P_{dc0} it is limited to P_{ac0}. This model for PV power production was used in paper (I).

Another model for PV power production, which was used in paper (VI), was developed in [5]. This model made use of solar irradiance data provided by the Meteonorm software for the location of Westminster, London (51°30′ N 00°08′ E) [170]. That model was based on input parameters such as temperature and PV system efficiency.

For paper (VII) the following model for PV power production was used. The PV power output was simulated from high-resolution incident solar radiation and the power output of the PV module was calculated from the formula:

$$P_{PV}(t) = \eta \times A \times G(t), \tag{3.37}$$

where $P_{PV}(t)$ is the power output over time t, A is the PV area (m^2), η is the efficiency of the PV system and $G(t)$ is the incident solar radiation (W/m^2). The system efficiency was set to $\eta = 13$ percent. The incident solar radiation data $G(t)$ was minute resolution, scaled from 5-second resolution data measured in a plane tilted 45° with a pyranometer at the Ångstrom Laboratory at Uppsala Sweden (59°50′19” N 17°38′50” E) during January 1 to December 31 2011.

In paper (IX) PV power production data was analyzed. This data represented meter values for PV power production for a number of locations over the duration of 281 to 310 consecutive days, depending on which solar charging station was measured.

3.3 Household electricity use

This section describes the household electricity use data and modeling which was used and developed in this thesis.

3.3.1 The Widén Markov chain model

In papers (IV), (VI) and (VII) the Widén Markov chain model for generating synthetic household electricity use data was used. This model was developed by Joakim Widén in [9, 10], and also extended to include EV home-charging in paper (IV), described in Section 3.4.1. For general information on Markov chain modeling, see Section 3.1.1.

The model was based on simulating activity patterns over time with a Markov chain and estimating electricity consumption via appliance use associated with each activity [9, 10]. In the model each Markov chain state was considered equivalent to an "activity" performed by an individual. The model was constructed based on the following two assumptions:

(I) Each individual occupies one state of activity at each time-step.
(II) The number of possible states is a fixed number.

Based on these assumptions and a large set of time-use data over activity patterns the probabilities for transition from one state to another in the Markov chain model were obtained [9, 10]. The model was based on the assumption that for each activity a certain set of appliances was used, and that when for example entering state "dishwashing" the dishwashing machine was started with a complex washing program in the background even if the state of activity of the resident was changed from the state "dishwashing" or not. The model was designed as bottom-up from an individual resident level so that a load profile was generated for each resident of the household. These load profiles where then added together with the exception of a "sharing scheme" which implied that certain appliances were shared among individuals, such as "TV" for example. If two or more residents in a household would happen to share for example the state "TV", then the electricity use of "TV" would only be that of one TV active, see [10, p.1882] for more detailed information.

The transition matrices were calibrated from a large set of Swedish activity data collected by Statistics Sweden (SCB), see [10, 72] for more information on activity categorization. The model was based on minute resolution with hour resolution transition matrices divided into categories of weekday and weekend day. The model also contained the option of simulating detached house or apartment. In order to obtain electricity use from activities an assumption of connection between states and appliance use was assumed together with a seasonal and diurnal dependent lighting scheme [9, 10]. In Table 3.3 the different states (activities) of the Markov chain model are given.

Table 3.3. *States and corresponding activities in the Markov chain model [10].*

State	Activity
1	Away
2	Sleeping
3	Cooking
4	Dishwashing
5	Washing
6	TV
7	Computer
8	Audio
9	Other

3.3.2 Probability distribution model

In paper (III) a probability distribution model representing household electricity use was developed. This section begins with a description of the model, and then moves on to describe the data set which was used to obtain the parameters for the PDFs in the model.

The model was designed for two system levels: Individual households and aggregates of households. Two assumptions defined the model:

(I) At any time, the magnitude of power demand for a household is a random outcome.
(II) The probabilities for all possible magnitudes of electricity use can be approximated by a continuous PDF.

Assumption (I) includes the random aspect of household electricity use. Assumption (II) suggests that household electricity use could sufficiently well — in approximation — be described by continuous PDFs. Together these principles set the stage for fit-to-distribution of electricity use data.

The model was developed according to the flow-chart in Figure 3.5. A description of the fit-to-distribution process in the model is illustrated in Figure 3.2 which include a histogram from a fictive data set and a fictive PDF calibrated with that data set.

Based on inspection of the histograms of the data sets Log-normal and Weibull PDFs were chosen since they appeared to capture the essential random features of the data sets. See Section 3.1.2 for details regarding the distributions. In order to include most of the diurnal and seasonal variation whilst keeping the number of distributions within a reasonable limit in the model, both Weibull and Log-normal distributions were obtained for the following categories:

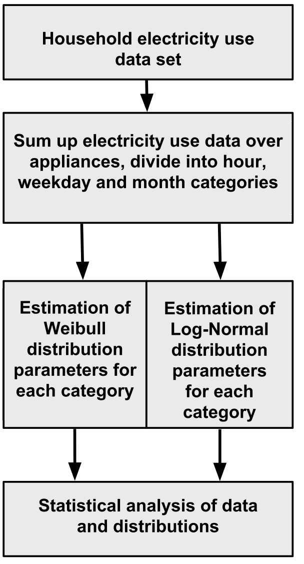

Figure 3.5. A flow chart of the process for developing the probability distribution model for household electricity use.

- Each hour of the day. (24)
- Each day of the week. (7)
- Each month of the year. (12)

This means in total 24 $\times$ 7 $\times$ 12 $\times$ 2 = 4032 probability distributions in the model, with an estimation of 8064 parameters in total. It should be noted that the data set had 10-minute resolution. The parameters of the distributions were calibrated with the aid of maximum likelihood estimates for each of the Weibull- and Log-normal PDFs, a method briefly described in Section 3.1.5. In practice MATLAB routines *wblfit* and *lognfit* were used for this purpose. Although the model was designed for modeling individual households it was possible to obtain PDFs for any number of households.

If one assumes that the power consumption in household i at time T is given by a stochastic variable X_i, then the electricity use of N households is the sum of the stochastic variables: $S_N = X_1 + X_2 + \ldots + X_N$, which constitutes a convolution of the distributions for stochastic variables X_i (cf. Section 3.1.3). If the household electricity use of each household in the aggregate of households can be considered independent, then for sufficiently many households it is possible to represent the household electricity use as a Normal distribution, according to the central limit theorem presented in Section 3.1.3.

It should be noted that the average electricity use of a few households might not be accurately represented by a Normal distribution like (3.20) since the central limit theorem is only necessarily true for large N [171].

In order to estimate goodness-of-fit of the model K-S tests were performed with original electricity use data on the one hand and a data set obtained from Monte Carlo simulations of the probability distribution model on the other. Given a significance level of e.g. $Q = 0.05$, the p-value is returned from the computation. Based on this a measure was defined as the ratio of "pass" relative to total number of distributions, corresponding to the number of categories, as was done in [171]. Results from this model are presented in Section 4.2.1.

The data which was used to obtain the distribution parameters in this model was thoroughly analyzed in [74], however that investigation did not include the development of any stochastic model based on the data, this was instead carried out in appended paper (III). The data was obtained from 400 households in Sweden: 40 of these households were measured for approximately one year and 360 households for approximately one month. Measurements were made on most of the appliances in each household (including heating when electric) on 10-minute resolution. Half of the data set was comprised of data from detached houses, the other half was data from apartments. In the study in paper (III) data for detached houses was used. This data set consisted of 200 households where 20 households were measured for a whole year and the rest for approximately one month. For more detailed information such as regarding residents, appliance specifications and electricity use see [74].

For this model certain assumptions regarding the data set were made. The goal of the study in paper (III) was to model household electricity use of an average household, and since the set of appliances were unique for each household the electricity use for each time-step was summed up for each household. Furthermore all electricity use data was divided up in categories for each hour, for each day of the week and for each month as described in the list of categories above. Each such category contains data from several different households, and it can be assumed that the data set is representative for the electricity use of detached houses in Sweden. The parameters of the probability distributions were obtained from the entire data set instead of for example dividing up the data set into training data and test data. This division can be found in machine learning theory, often applied if there is a classification issue, while the objective of this study was to fit probability distributions to data.

3.4 Electric vehicle charging

In this section the methodology for EV charging modeling is described. Two types of EV charging models were developed in papers (IV) and (V). In paper (IV) a Markov chain model was developed and in paper (V) a probability distribution model was developed. Both models are stochastic, but based on two different types of methodology. In paper (VIII) these models were combined to make a probability distribution model of EV home-charging which in turn was used in combination with the probability distribution models for PV power production published in paper (I) and household electricity use in paper (III).

3.4.1 Electric vehicle Markov chain model

Based on the Widén model for generating synthetic household electricity use an EV extension for estimating the electricity consumption from a home-charged EV was developed in paper (IV). This EV extension connects the synthetic activity patterns for residents in a household with EV use and consequent charging. Although this extension is based on the Widén model, it is also based on additional principles:

(I) The EV is used by one fixed resident in the household during a certain percentage of the states "Away" for that individual.
(II) The choice for the fixed resident to take the EV is with the probability in (I) made each time the state changes to state "Away". This choice is kept for every time step after this which is not changed from state "Away".
(III) The EV electricity consumption is proportional to the EV's time away until the state of charge ($SOC(t)$) reaches the minimum state of charge SOC_{min}.
(IV) If the EV is away for longer time than is possible with the limited battery capacity, thus reaching the minimum state of charge (SOC_{min}) before the trip is completed, then the EV is assumed to have paused during the trip or run on some other fuel during the remaining part of the trip (if it is a PHEV).
(V) The EV is only charged when at home and not fully charged.

Formally this model follows the mathematical structure of the Widén Markov chain model described in Section 3.3.1. According to principles (I) and (II) there is a certain probability $\mathscr{P}_{EV}$ that the EV is used by a resident when the resident state is changed to the state "Away", see Table 3.3 for a list of states in the Widén model. According to principle (III) the EV consumes a constant amount of electric power during each time step when away, but according to principle (IV) this is only true for as long as the minimum state of charge SOC_{min} is not reached. For trips with longer duration than there is battery state of charge for — according to this setup — there is an assumption that the EV stopped during the trip and depleted the state of charge upon arrival home. Another interpretation of this scenario is that the EV has some other on-board engine (for example an ICE) which provides the energy for the remainder of the trip.

The state of charge of the battery is given by $SOC(t)$ at time t. When fully charged the state of charge is at a maximum level $SOC(t) = SOC_{max}$. When the EV is used then according to principle (III) the state of charge is decreased linearly with an electricity consumption of C^{EV} times the seasonal coefficient $S(t)$, until it is depleted to the minimum depth of discharge (DoD), which is here modeled as a minimum state of charge SOC_{min}, or returned home (as the state has changed from "Away" to some other). Upon arrival at home the EV is immediately plugged in and charged according to principle (V). The EV is charged with charging power C^{Charge}, which in practice increases $SOC(t)$ until some time step τ for which $SOC(\tau)$ equals SOC_{max}. With time-step Δt this can be expressed via the following equation:

$$SOC(t+\Delta t) = \begin{cases} SOC(t) - C^{EV} S(t)\Delta t & \text{if consuming,} \\ SOC(t) + C^{Charge}\Delta t & \text{if charging,} \\ SOC(t) & \text{else.} \end{cases} \tag{3.38}$$

The level of charge C^{Charge} is dependent on which type of charging is used. The EV extension also has to ensure that the state of charge is kept within the accepted limits:

$$SOC_{min} < SOC(t) \leq SOC_{max}. \tag{3.39}$$

The parameters and nomenclature is listed in Table 3.4. The results for this model in combination with household electricity use is given in Section 4.3.1.

Table 3.4. *Parameters for the Markov chain EV home-charging extension.*

Description	Parameter
Maximum state of charge [kWh]	SOC_{max}
Minimum state of charge [kWh]	SOC_{min}
Charging power [kW]	C^{Charge}
Electricity consumption [kW]	C^{EV}
Probability to take the EV [%/100]	$\mathscr{P}_{EV}$
Average driving velocity [km/h]	V
Driving electricity consumption [kWh/km]	ν
Seasonal coefficient [%/100]	$S(t)$

Upon arrival at home the EV is assumed to be immediately connected to the grid and charged with C^{Charge} until the the maximum state of charge SOC_{max} has been reached or the EV is taken out driving again. This grid interaction is described by:

$$P_{EV}(t) = \begin{cases} C^{Charge} & \text{if charging,} \\ 0 & \text{else.} \end{cases} \tag{3.40}$$

The seasonal variation in fuel consumption for the standard setup is a factor $S(t)$ times the average fuel consumption. For the different seasons these factors in appended paper (IV) were set according to the following values: Winter: $S(t) = 1.2$, spring: $S(t) = 1$, summer: $S(t) = 0.8$, fall: $S(t) = 1.0$.

The seasonal coefficient adjusts the variability of load from vehicle use from seasonal conditions from for example heating.

3.4.2 Electric vehicle probability distribution model

In addition to the Markov chain model for EV charging a probability distribution model was developed in paper (V). First the model will be described, then a description of the data set which was used to calibrate the model follows.

This model was based on Bernoulli probability distributions and a maximally opportunistic charging scheme; charging every time the vehicle stopped. The model was set up according to the schematic illustration in Figure 3.6.

While there are many different types of probability distribution models for EV charging a Bernoulli distribution approach, calibrated with data on driving patterns in Sweden, offered a simple framework for charging based on assuming charging at every stop. In this way variability of charging and average charging patterns could be obtained.

This setup is based on a number of assumptions. The assumption is that the probability for being out driving an EV is similar to the probability for being out driving an ordinary vehicle. Hence it is assumed that data for driving an ordinary vehicle can be used as a basis for determining the driving behavior of an EV. Second one can assume that probability distributions for a feasible charging pattern can be reasonably estimated from Monte Carlo simulations based on the probabilities for being out driving together with a simple model of the EV with a given battery size, average fuel consumption and charging power. Also, for simplicity, it is assumed that the charging is binary: no charging or full charging at each time step (10 minutes resolution, see below).

Finally, in similarity with the EV Markov chain model, the assumption is that when the EV is not being driven it is charged until fully charged or taken out driving again. These assumptions suggest that the model ideally represents shorter EV-trips, typically within a city. The short distance approximation in this model is related to the time-step resolution, so a 10 minute time-step — that is a 10 minute typical trip length — is reasonable. It should be noted that from these probability distributions it is possible to for example estimate expected values for electricity use or use Monte Carlo simulations in order to obtain a time series for charging. Also, an model based on Bernoulli probability distributions is a general concept and could be applied to time series of charging under the assumption of binary charging: only full charging or no charge. This was done using data for home-charging from the Markov chain EV charging model in paper (IV) in order to represent home-charging on a probability distribution basis for paper (VIII).

The first step of the model is to estimate the probabilities for driving compared with not driving from a time-use data set for Sweden [172]. This was done for the following categories:

- Each hour of the day (24)
- Week day/Weekend day (2)

This categorization of in total 2×24 distributions was chosen in order to obtain enough data so that each distribution represented actual driving habits accurately within reasonable limits, while maintaining a level of resolution in the model which represents sufficient data for estimating realistic and applicable charging patterns. The time-use data was collected on five-minute basis for week day and weekend day [172]. For each category there was between 4860 and 5172 data points. The data set was obtained from 926 time-use diaries from 464 persons in 179 households in a Statistics Sweden pilot study from 1996 [72, p.45]. These individuals reside in households with different setup (e.g. couples, singles, with and without children), and the survey included both apartments and detached houses [172]. The resolution was five-minute and the data was based on activities, later categorized via "activity codes”. In this data set one particular activity was classified as "vehicle driving". The frequency of this subset of data for each household was used to obtain the parameters for the probability distributions. The model setup is shown in Figure 3.6.

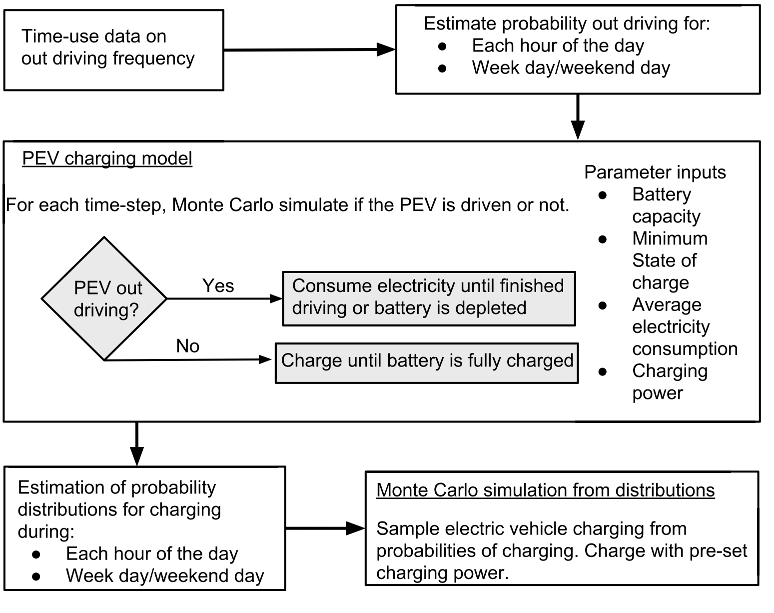

Figure 3.6. A flow chart of the EV charging probability distribution model.

Formally, from the time-use data the probability $p_{use}(t)$, for using the EV or not, was obtained for the categories of time detailed above. The next step was to perform a Monte Carlo random sample using the estimated probability $p_{use}(t)$ (use the EV or not). The state of charge over time in the model was determined with the same setup as for the Markov chain model for home-charging in (3.38), but with the seasonal faction $S(t) = 1$ for all seasons. This implies that the state of charge decreases when out driving and gets replenished until fully charged or taken out driving again. Here C^{EV} is the average electricity consumption when being driven, and C^{Charge} is the charging power. Δt is the time-step of the simulation; set to ten minutes in the paper. In order to have a reasonable battery life expectancy the battery was restricted from dropping below a minimum state of charge SOC_{Min}. The setup of the paper (V) was $SOC_{Min} = 0.6 \times SOC_{Max}$. When the EV was not in an "being driven" state it was charged, and the grid interaction was defined in the same way as for the Markov chain EV home-charging model in (3.40). This represented the grid interaction of the EV charging. When performing simulations to obtain data series for a large number of weeks it was possible to quantify the probability distributions of charging for the following categories (the same type of categories as for the distributions of being out driving in the list above):

- Each hour of the day (24)
- Week day/Weekend day (2)

A nomenclature of parameters is found in Table 3.5. It should be noted here that the battery model used in this EV charging model is the same battery model as was used in the Markov chain EV home-charging model described in Section 3.4.1. This distribution model could perhaps be characterized as maximally opportunistic since the EV is always connected and charged when it stops, even though the state of charge might be high and there is no necessity for charging.

Table 3.5. *Parameters in the EV distribution model.*

Description	Parameter
Electricity consumption [kW]	C^{PEV}
Charging power [kW]	C^{Charge}
Maximum battery charge [kWh]	SOC_{Max}
Minimum state of charge [kWh]	SOC_{Min}
Average driving velocity [km/h]	V
Driving electricity consumption [kWh/km]	v

The probability distribution setup for charging is discussed in the following section.

In similarity with the probability distribution approach to clear-sky index in paper (II), described in Section 3.2.4, this model utilizes a Bernoulli distribution approach. The Bernoulli PMF was introduced in Section 3.2.4, but the EV charging application of Bernoulli distributions will be described more in detail in this section.

If one assumes that there is a probability p at a time-step for charging, and thus probability $1-p$ for not charging at that time-step, a natural setup is a Bernoulli distribution.

The model is defined by the probability of charging or not charging, this means that the electricity use Q could be modeled by a stochastic variable $X \sim \text{Bernoulli}(p)$ with a weight for power use C^{Charge}:

$$Q = C^{Charge} X. \tag{3.41}$$

This setup can then be used for Monte Carlo simulations of electricity use, but as a probability distribution it could for example directly be used to calculate the electricity use of several uncorrelated EVs. If one generalizes (3.41) the electricity use Q_N from N uncorrelated EVs is:

$$Q_N = C^{Charge}(X_1 + X_2 + \cdots + X_N) \tag{3.42}$$

where $X_i \sim \text{Bernoulli}(p)$. This power use can be calculated analytically directly from the convolution of Bernoulli distributions [173] (See Section 3.1.2):

$$\sum_i^N X_i \sim \text{Bin}(N, p). \tag{3.43}$$

Furthermore since for large N it is possible to approximate the discrete probability distribution in (3.43) with a normal distribution if one assumes that the mean value $\mu = Np$ and variance $\sigma^2 = Np(1-p)$ holds for the Normal distribution:

$$\text{Bin}(N, p) \sim \text{Normal}(Np, Np(1-p)). \tag{3.44}$$

Results for the probability distribution model of EV charging is presented in Section 4.3.2.

3.5 Solar charging station data

In collaboration with the Swedish company Solelia Greentech AB we were able to quantify and investigate PV power production and EV charging from a set of eight solar-charging stations distributed across Sweden. Each solar charging station consisted of an EV charging station and an adjacent PV power production facility owned and operated by companies or municipalities. All systems were connected to the so-called "solar bank", a concept and a technological infrastructure system that stores data on EV charging and PV power production for the purpose of obtaining and transferring guarantees of origin (GO:s) for the PV power production and EV charging.

The eight solar charging stations in the study were located in pairs at four sites: Eskilstuna city center, Uppsala city center, Marieberg mall in Örebro and in Gothia Science Park in Skövde. Each site contained eight Yingli 240p-29b PV panels with a peak power of $8x240$ W_p along with two EV charging outlets based on 2.3 kW AC (230V, 10A) power.

In order to compare power production with power consumption the PV power production is evenly divided in two so that there is both electricity consumption and production at each station, not just one for each pair. Thus each charging outlet and adjacent PV power production system was defined as a station in this setup.

The data was comprised of separate meter-data for EV charging and PV power production for each site. The data sets are based on minute resolution for each station for between 281 and 310 consecutive days depending on site. Results from the data analysis of the solar charging stations are presented in Section 4.5.2.

3.6 Grid interaction

There are different indicators of self-consumption which were used and developed for this thesis and papers (VI), (VII), (VIII) and (IX). These will be described here.

3.6.1 The complete model

In order to investigate the interaction of the models for PV power production, household electricity use and EV charging a complete model framework was developed. The power consumption/production at the end-user in the grid for the individual household level with PV power production $P_{PV}(t)$, household power consumption $P_{Household}(t)$ and EV home-charging power consumption $P_{EV}(t)$ over time t can be expressed in a single equation:

$$P(t) = P_{PV}(t) - P_{Household}(t) - P_{EV}(t). \tag{3.45}$$

In this equation negative power production means in practice power consumption. With this complete model given any data — modeled or measured — it is possible to quantify the total electricity consumption/production at the end-user. For an aggregate of N households (3.45) is generalized to:

$$P(t) = \sum_{i}^{N} (P_{PV,i}(t) - P_{Household,i}(t) - P_{EV,i}(t)). \tag{3.46}$$

This complete model was utilized in papers (VI) and (VII) with the aid of the Widén Markov chain model for household electricity use (see Section 3.3.1), EV Markov chain home-charging (see Section 3.4.1) and PV power production (see Section 3.2.6). The complete model was also outlined in the not appended publication (XVI). A flowchart for the complete model presented in Figure 3.7. Results for the complete model is presented in Section 4.4.1.

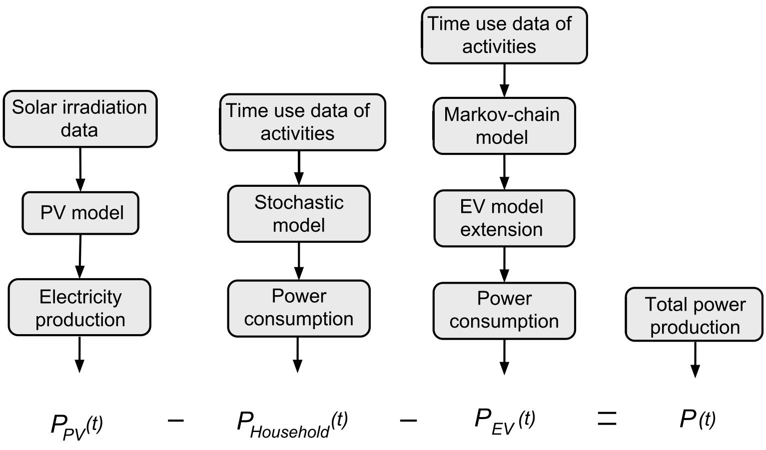

Figure 3.7. A schematic illustration of the complete model connecting PV power production, household electricity use and EV home-charging which was used in paper (VII).

In paper (III) the complete model was generalized to using stochastic variables. A stochastic generalization of (3.45) representing power production over time is given by:

$$X = A \times X_{PV} - X_{Household} - X_{EV}, \tag{3.47}$$

where X_{PV} represents the bimodal Normal probability distribution-based stochastic variable (see Section 3.2.2) with PV area A. $X_{Household}$ represents the Weibull probability distribution-based model stochastic variable (see Section 3.3.2) and X_{EV} represents the EV Bernoull probability distribution-based stochastic variable described in Section 3.4.2 but calibrated with home-charging from the EV Markov chain model 3.4.1. This calibration uses a power consumption profile generated from the Markov chain EV home-charging model and sets up Bernoulli probability distributions for charging during each hour of the day for weekday and weekends. A flowchart for the complete model based on stochastic variables is presented in Figure 3.8.

The grid interaction equation (3.47) corresponds to a convolution of the probability distributions for the stochastic variables corresponding to PV power production, household power consumption and EV charging. This convolution was numerically computed in paper (VIII). The complete probability distribution model can also be generalized to N households, which corresponds to a

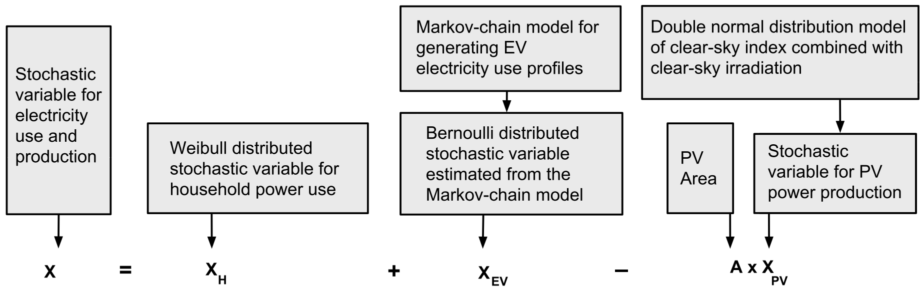

Figure 3.8. A schematic illustration of the complete probability distribution model connecting PV power production, household electricity use and EV home-charging which was developed in paper (VIII).

convolution of the distribution of each household:

$$X_N = \sum_{i}^{N} \Big(X_{PV,i} - X_{Household,i} - X_{EV,i} \Big). \tag{3.48}$$

It should be noted here that while the central limit theorem applies to convolutions of variables, a requirement is that the variables are not dependent, which is generally not the case for the stochastic variable setup in (3.48). Results for the complete probability distribution model will be given in Section 4.4.2.

3.6.2 Solar and load fractions

Two useful measures of self-consumption were used in papers (VII) and (IX): Solar fraction (SF) as the fraction of load covered by PV power production, and load fraction (LF) as the fraction of PV power production covered by load. For alternative nomenclature and measures see [37].

Since SF is defined as the fraction of load that is matched with PV power it can mathematically, together with the nomenclature described in the illustration in Figure 3.9, be represented as:

$$SF = \frac{B}{A+B+C}. \tag{3.49}$$

Conversely, LF is defined as the fraction of PV power which is matched by load, which can then also be defined mathematically as:

$$LF = \frac{B}{B+D}. \tag{3.50}$$

It should be noted that for NZEBs the solar fraction equals the load fraction since the parts $A+B+C$ and $B+D$ under those circumstances are equal. In similarity with the time series based estimates for evaluating solar fraction

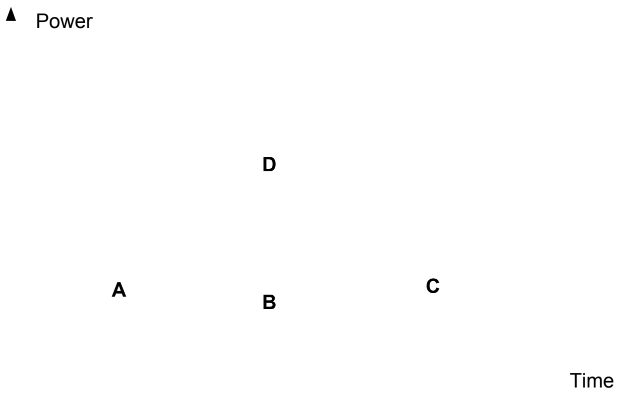

Figure 3.9. A schematic illustration of a load curve (solid) and production curve (dashed) with appropriate labels for energy that is used to obtain solar and load fractions.

and load fraction it is possible to use a stochastic variable approach instead. In such an approach SF and LF become stochastic variables based on (3.49) and (3.50), but with A,B,C and D as stochastic variables. For an applicable mathematical model for estimating SF and LF from time series of power consumption and production, see not appended paper (XVI).

In this thesis distributions for SF and LF were determined via time series generated by Monte Carlo simulations of each component in paper (VIII). With the use of time series for load and production (3.49)-(3.50) can be used to estimate time series for SF and LF, which in turn can be used to make histograms. Results for this is presented in Section 4.4.2.

4. Results

In this chapter the results are presented. In Section 4.1 results regarding PV power production are presented and in Section 4.2 results regarding household electricity use are given. In Section 4.3 results for EV charging are presented and finally in Section 4.4 results regarding self-consumption and grid interaction are given.

4.1 Photovoltaic power production

This section presents results from the studies on solar irradiance and PV power production in papers (I) and (II).

4.1.1 Bimodal probability distribution model

The bimodal Normal probability distribution model for solar irradiance and PV power production was developed in paper (I), and described in Section 3.2.2. In Figure 4.1 histograms of clear-sky index and calibrated PDFs are given for each tested setup of unimodal, bimodal and trimodal Normal distributions. The left-most plot shows unimodal Normal fit, then bimodal Normal fit and finally a trimodal Normal fit is given to the right.

In order to ascertain goodness of fit Kolmogorov-Smirnov tests were performed for the unimodal Normal, bimodal Normal and trimodal Normal distributions and obtained the following test-values: 0.4740, 0.4498 and 0.4503 respectively. The bimodal Normal distribution has the lowest K-S value, which indicate that it is best fit. Overall the K-S test values are relatively low for all distributions, which is probably related to the lack of smoothness in the histogram of the clear-sky index. With the Expectation-Maximization (EM) algorithm the parameter setup for a bimodal Normal distribution fit to these data is presented in Table 4.1.

It should be noted that most weight is put on the distribution with mean μ_1 (at lower values) while the distribution with mean μ_2 has a smaller standard deviation.

One of the main aims of the study in paper (I) was to obtain the clear-sky index and PV power production for dispersed uncorrelated locations by defining and investigating an aggregate clear-sky index. In this process the aggregate clear-sky index was shown to be normally distributed for five or

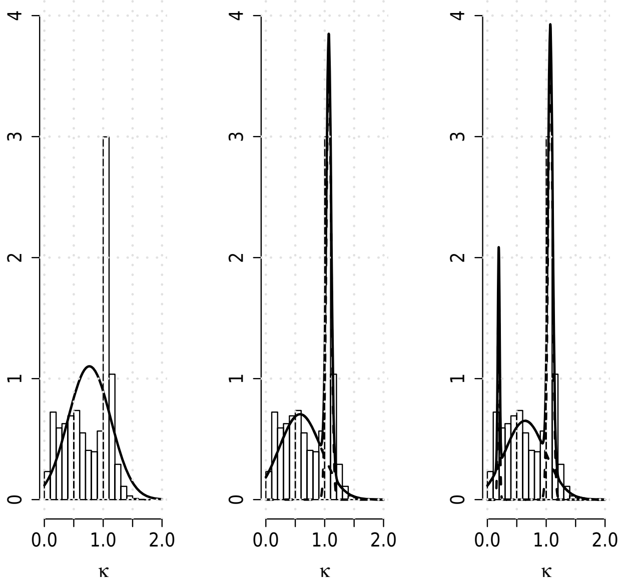

Figure 4.1. Histograms of the clear-sky index data described in Section 3.2.2 along with calibrated distributions: unimodal Normal distribution (Left), bimodal Normal (Middle) distribution and trimodal Normal distribution (Right).

Table 4.1. *Estimated parameter values for the bimodal Normal distribution of clear-sky index using* (3.26).

μ_1	μ_2	σ_1	σ_2	w_1	w_2
0.58	1.07	0.35	0.04	0.63	0.37

more dispersed locations. Since the locations were assumed to be dispersed enough to be uncorrelated the distribution of the average aggregate clear-sky index follows the central limit theorem and is by inspection approximately $\mathcal{N}(\mu, \sigma/\sqrt{N})$. As an example this is shown for various numbers of dispersed locations in Figure 4.2.

This simplifying method was analyzed in terms of usefulness, in terms of application to PV power production, by quantifying the deviation on a tilted plane between making the conversion from the horizontal to the tilted plane for each location separately and for the aggregate clear-sky index. With the Erbs model for estimating PV power production on a tilted plane, described in Section 3.2.5 PV power production was obtained for two cases: horizontal plane and 40 degrees tilt. The resulting daily power production for these cases

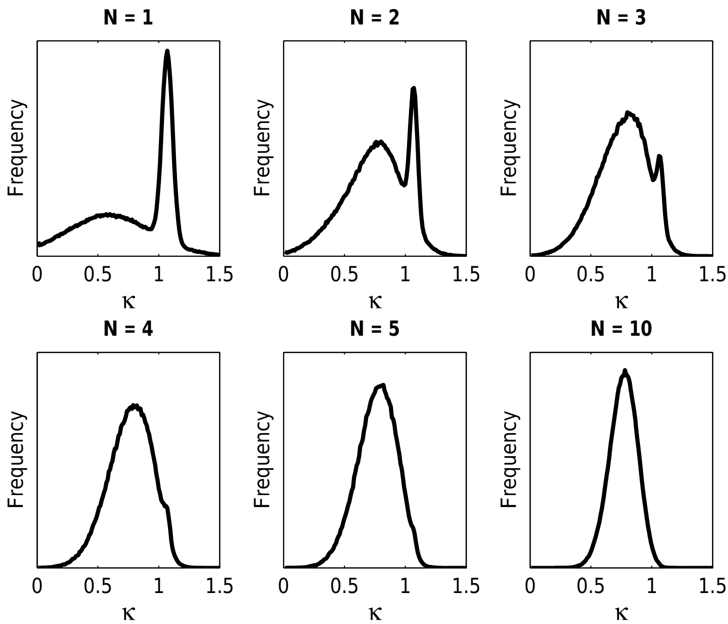

Figure 4.2. Line plots based on histograms of the simulated average aggregate clear-sky index for *N* dispersed locations by using the bimodal Normal distribution of single location clear-sky index.

on one typical moment during one typical day is shown in Figure 4.3. The parameter values in the PV power production model is shown in Table 4.2.

Table 4.2. *Setup on the PV power production model connected to the bimodal Normal distribution model for clear-sky index.*

v_m	q_a	A	ρ_q	P_{ac0}	P_{dc0}	P_{s0}
15 %	15 %	10 m^2	20 %	1500 W	1550 W	15 W

The line plots based on histograms for aggregate horizontal mounted PV power production show that PV power production is the same when using the aggregate clear-sky index compared with using an average of PV power production for each location. When the PV power system was inclined (here 45 degrees) the results from the two approaches diverge.

This deviation stems from the impossibility to properly separate direct and diffuse components of the solar irradiance when using only the aggregate clear-sky index. This is not an artefact of the model, instead this can be traced to the loss of information inherent to the convolution process of the aggregate clear-sky index. The index loses information in the convolution process since the state of cloudiness for each location is averaged and the separation of beam- and diffuse components of clear-sky index for inclined plane power production calculations is not longer possible to perform correctly. Instead the aggregate clear-sky index serves as an approximation for multiple dispersed locations, typically if no other information is available.

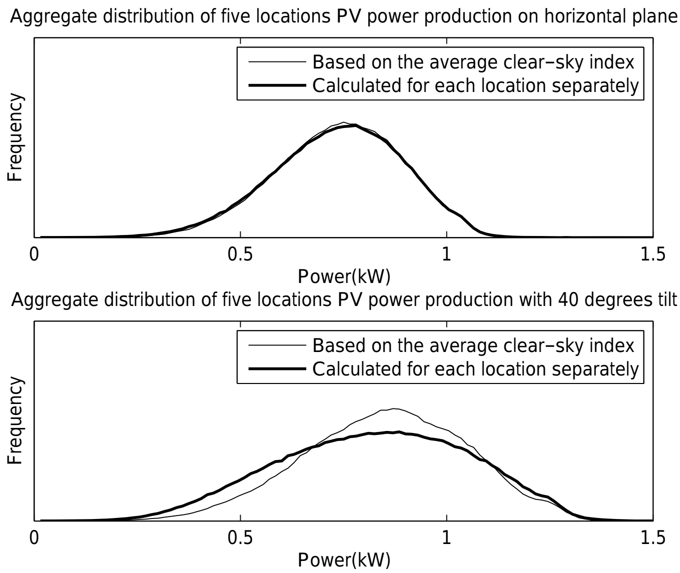

Figure 4.3. Line plots based on histograms of aggregate PV power production from the aggregate clear-sky index and aggregate PV power production simulations from the model of PV power production for each location. PV power output in both scenarios are shown for zero and 40 degrees tilt facing south for one minute on one arbitrary summer day: 12:00 on June 19.

4.1.2 Convolution approach

A convolution approach to modeling solar irradiance was introduced in paper (II), and described in Section 3.2.4. Here the data and the fit-to-distribution results are shown along with the derivation of a generalized Ångström equation.

In paper (II) data for DHI and BHI was obtained for the location of Norrköping, see Section 3.2.4 for more information on the setup. Histograms along with the calibrated probability distributions for DHI and BHI with scaling parameter $\beta = 0.69$, a consequence of using a threshold of $\sigma = 0.01$, are shown in Figure 4.4.

It has proven possible to empirically estimate solar irradiation from the number of bright sunshine hours relative to clear-sky irradiance, as was first investigated in [174] and [38, 39]. This can be expressed as the Ångström equa-

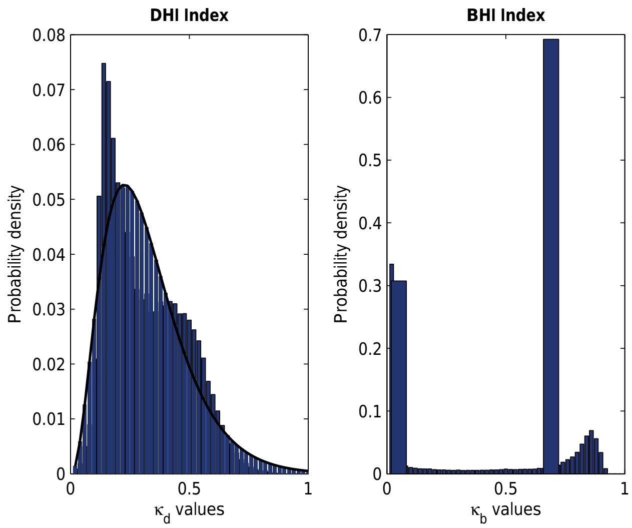

Figure 4.4. Histograms and fit-to-distributions for the DHI clear-sky index, corresponding to a Gamma distribution, and the BHI clear-sky index corresponding to a weighted Bernoulli distribution.

tion relating average solar irradiance to duration of bright sunshine [39, 165]:

$$\frac{\bar{G}}{\bar{G}_c} = \alpha + (1-\alpha)S. \tag{4.1}$$

Here $\bar{H}$ is the monthly average of daily horizontal surface radiation, $\bar{H}_c$ is the average daily clear sky solar radiation, $S \in [0,1]$ is the fraction of bright sunshine and α is a parameter for each location.

Based on the setup of the convolution model in Section 3.2.4 the following can be concluded regarding expected values of the convolution approach. GHI is, by definition, the clear-sky irradiance weighted by the clear-sky index according to (see Section 3.2.4 for nomenclature):

$$G = (X_d + X_b)\, G_c, \tag{4.2}$$

where G and G_c are now considered stochastic variables as well. Recall from (3.29) that $X_b = \beta X_b'$, where β is a constant, then one gets the following expected value of (4.2):

$$E[G] = E[(X_d + X_d)G_c] = E[X_d + \beta X_b']E[G_c], \tag{4.3}$$

where one can identify the ratio of monthly average daily horizontal irradiance $\bar{H}$ and the monthly average of clear-sky irradiance $\bar{H}_c$ via the ratio of expected values for G and G_c:

$$\frac{\bar{H}}{\bar{H}_c} \equiv \frac{E[G]}{E[G_c]}. \tag{4.4}$$

Despite X_d and X_b are correlated, the expected value of the sum of X_d and X_b is equal to the sum of the expected values, which brings the following expression:

$$\frac{\bar{H}}{\bar{H}_c} = E[x_d] + \beta E[x_b']. \tag{4.5}$$

It is known that $E[X_d] = \gamma\delta$ is the expected value of the Gamma distribution (3.12). Here this represents the average solar irradiance from cloudiness. $E[X_b']$ is the expected value of the Bernoulli distribution:

$$E[X_b'] = p. \tag{4.6}$$

This brings a generalization of the Ångström equation (4.1) for estimates of solar irradiation:

$$\frac{\bar{H}}{\bar{H}_c} = \gamma\delta + \beta p \tag{4.7}$$

where one can identify $\gamma\delta \sim \alpha$ and $p \equiv S$ in the Ångström equation (4.1), but β is not necessarily equivalent to $1-\alpha$, which defines the generalization of the Ångström equation. It should be pointed out that (4.7) is similar to the empirical Ångström-Prescott equation with the difference that the Ångström-Prescott equation is based on extraterrestrial radiation instead of clear-sky irradiance [165, 175]. With data on DHI and BHI from one year (2008) solar irradiance measurements for the location of Norrköping, Sweden (59°35′31” N 17°11′8” E) [158], along with proper fit-to-distribution routines for the data set outlined in Section 3.2.4, one arrives at: $\gamma\delta = 0.32$ and $\beta = 0.64$. It should be noted that value of β is achieved with a threshold of $\sigma \sim 0.01$.

These estimates can be compared with Ångström's original results for Stockholm, Sweden in 1924: $\alpha = 0.25$ (compared with $\gamma\delta = 0.32$)), $1-\alpha = 0.75$ (compared with $\beta = 0.64$) [39].

4.2 Household electricity use

This section shows results for household electricity use based on the probability distribution model developed in paper (III). Results for the Widén model are not given explicitly in this thesis, since the model was previously developed, validated and analyzed by Joakim Widén [10]. Instead it is compared with the probability distribution model in Section 4.2.2 and in connection with the Markov chain EV charging model in Section 4.3.1.

4.2.1 Probability distribution model

The probability distribution model for household electricity use is described in Section 3.3.2. Based on a large data set on electricity use from detached houses in Sweden Weibull and Log-normal probability density distributions were calibrated for different time-bins for each hour, each day of the week and each season. Unlike the Widén model this model contains electric heating as well. As an example of the output from the model a Weibull probability distribution of power consumption for each hour of the day during winter time is shown in Figure 4.5.

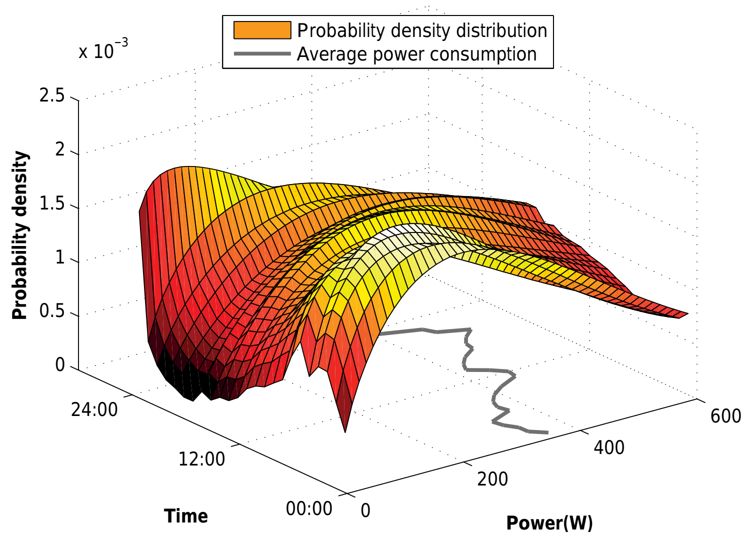

Figure 4.5. A surface plot of Weibull probability density distributions representing electricity use for each hour on Mondays during winter time, generated from the household electricity use probability distribution model from paper (III). The gray line situated in the power-time plane represents the average power consumption for each hour of the day. This surface plot is also present on the front page of the thesis.

From this figure it is possible to determine that the average power consumption is highest during late evening, but with a minor spike during noon. A minimum is reached around 05:00 in the morning. The more pronounced the peak is in probability density the lower the variability of power use, it is thus noticeable that the midnight variability appears to be lower than the daytime variability. This is presumably related to the variability in activities during daytime, which is mostly lacking during nighttime.

4.2.2 Comparison of models

The Widén Markov chain model for household electricity use was used in papers (IV), (VI) and (VII). The Weibull probability distribution model was developed in paper (III) and also used in paper (VIII). In this section these models are compared. The year average diurnal power consumption is shown in Figure 4.6.

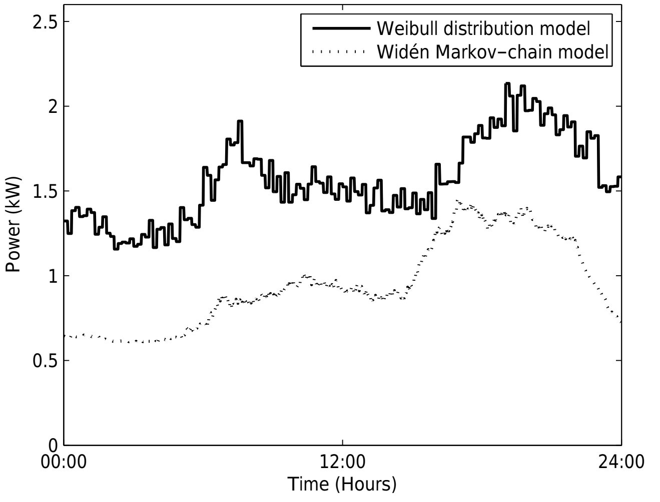

Figure 4.6. Year-average power consumption simulated from the Weibull probability distribution model compared with a five resident detached house simulation in the Widén model. Both models are simulated with minute resolution.

The Widén Markov chain model was designed to produce time series of electricity use from activities based on probabilities for changing activity and electricity use associated with each activity. In comparison the probability distribution model is primarily designed to characterize electricity use in terms of PDFs, but also secondarily to be able to produce time series of electricity use. This implies that the Markov chain approach produces perhaps more realistic time series, while the probability distribution model gives more applicable analytic expressions quantifying the variability of electricity use.

The total yearly electricity use estimated by the Weibull probability distribution model for detached house setup is 13.7 MWh and for the Widén Markov chain model with five residents and detached house setting it is 8.3 MWh. One major difference between the models is that the probability distribution model is fit-to-distribution directly on a large data set of electricity use for detached Swedish houses whereas the Markov chain model is based on activities and assumes electricity use for each activity and background appliances such as refrigerator. The probability distribution model then represents an average type of household in the data-set whereas the Widén model has free variables, such as the number of residents. The main model-setup difference in terms of estimated energy consumption is the inclusion of electric heating in the probability distribution model. This is the main factor in the difference in yearly electricity use. It should be noted that the Widén model was validated with the same electricity use data provided by the Swedish Energy Agency which was used to calibrate the distributions in the household electricity use probability distribution model, see [74] for more information on the data set. This similarity is reflected in the profiles of the year average diurnal load shown in Figure 4.6, where on average both models have a high base load, a peak in consumption during morning and a larger peak in the evening.

4.3 Electric vehicle charging

A Markov chain model for EV home-charging was developed in paper (IV) and a probability distribution model of EV charging was developed in paper (V). Results for the EV home-charging model, which was an extension to the Widén-model for household electricity use, is presented in Section 4.3.1. Results for the probability distribution model for EV charging is presented in 4.3.2.

4.3.1 Electric vehicle Markov chain model

This model was developed in Paper (IV). It was also used in paper (VI) as a basis for estimating EV charging in the City of Westminster and in paper (VII) for estimating the correlation between PV power production and EV charging.

This EV charging model was designed to be a home-charging model (see Section 3.4.1). As an example one may setup the Widén model with two residents in a detached house and one home-charged EV. The free parameters of the EV are setup to match the specifications of Tesla model S combined with standard driving behavior used in paper (IV), see parameters in Table 4.3.

Table 4.3. *Simulation setup on the Markov chain EV home-charging model.*

C^{Charge}	C^{PEV}	$\mathscr{P}_{PEV}$	SOC_{min}	SOC_{max}	D	V	v
2.3 kW	8.4 kW	0.2	0 kWh	85 kWh	37 km	46km/h	0.2 kWh/km

A combination of model output for household electricity use and EV home-charging is presented in Figure 4.7. The corresponding yearly electricity use for this setup is given in Table 4.4.

In this simulation the total electricity use from the two resident detached house excluding any form of electric heating is 4.13 MWh/year and the EV charging is 5.60 MWh/year. Keep in mind here that the EV model is limited to one resident as driver of the EV. Figure 4.7 shows a large power consumption on average during the day, but with a pronounced peak during evening and

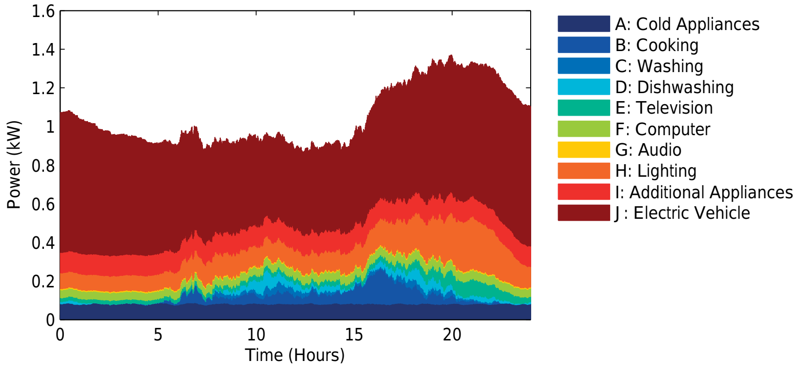

Figure 4.7. A stacked bar-plot over year average daily power consumption from appliance categories and a home-charged EV with specifications in Table 4.3. The corresponding electricity use from each category of appliances is given in Table 4.4.

Table 4.4. *Electricity demand (MWh/year) from the Widén model with the EV home-charging extension. Nomenclature list is given in Figure 4.7.*

A	B	C	D	E	F	G	H	I	J
0.72	0.33	0.09	0.20	0.28	0.39	0.06	1.13	0.93	5.02

nighttime. This model is further investigated in connection with PV power production in Section 4.4.1.

4.3.2 Electric vehicle probability distribution model

In this section simulations of the EV probability distribution model are presented. In similarity with the simulations for the Markov chain EV home-charging model this model is also setup with Tesla Model S specifications for these simulations. The parameter setup is shown in Table 4.5 and a year average daily power consumption profile is given in Figure 4.8.

Table 4.5. *Setup on the EV charging probability distribution model, for nomenclature see Table 3.5.*

C^{Charge}	C^{PEV}	SOC_{min}	SOC_{max}	V	v
2.3 kW/11 kW (fast)	8.4 kW	0 kWh	85 kWh	46 km/h	0.2 kWh/km

The result indicates an average power consumption peak in the morning and a larger average peak in power consumption in the evening. The model predicts a total yearly electricity use of 2.2 MWh. Overall the introduction

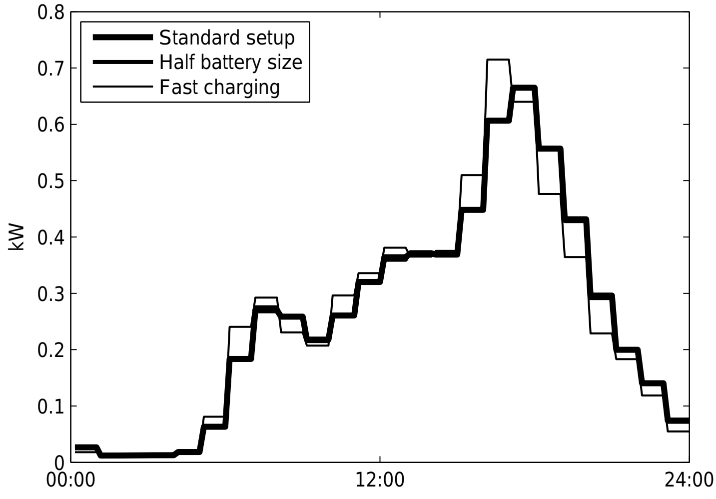

Figure 4.8. A year average daily power consumption profile for EV charging simulated via the EV charging probability distribution model with setup from Table 4.5. Note that the half-battery size is hidden behind the power consumption profile of the standard setup. This is because the half-battery capacity setup has a negligible impact in this maximally opportunistic charging setup, which charges often.

.

of fast-charging of 11 kW instead of 2.3 kW merely shifts the average load profile in time, with slightly higher peak but no significant difference in energy use. The most striking feature is perhaps the lack of an effect of reducing the battery capacity to half, from 85 kWh to 42.5 kWh. This is because of the maximally opportunistic setup of the model. By assuming that it charges whenever stopped the EV has a tendency to charge often, which means that the battery is rarely depleted, even if having a low capacity. This also emphasizes the short-trip limit — typically city trips — applicability of the model. It can also be seen as a model for the intermediate step between charging at a few locations (such as only at home) and a completely electrified infrastructure.

4.3.3 Comparison of models

The similarities and the differences between the Markov chain model for EV home-charging and the Bernoulli probability distribution model for maximally opportunistic EV charging can be quantified in terms of electricity use and average daily variability. In Figure 4.9 year average diurnal plots of power consumption for the standard setup of the Markov chain EV home-charging model and the maximally opportunistic Bernoulli distribution EV charging model are presented. The setup is presented in Tables 4.3 and 4.5 with the exception of using a smaller available battery capacity of 14 kWh in order to put the models on par with a relatively short-range EV.

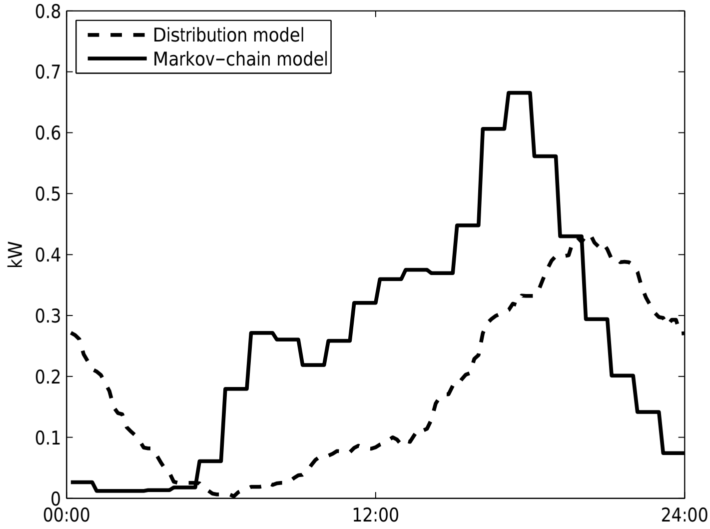

Figure 4.9. Year average diurnal variability of EV charging from the Markov chain model for EV home-charging and the Bernoulli probability distribution model for maximally opportunistic EV charging at any place. Both models were setup with parameters in Tables 4.3 and 4.5 with the exception of using 14 kWh for both models in order to put the models on par with a relatively short-range EV setup.

.

The probability distribution model had an energy consumption of 6.2 kWh/day or 2.3 MWh/year while the Markov chain model had 4.3 kWh/day or 1.6 MWh/year, which suggests that maximally opportunistic charging uses more energy with the same setup. Although this is a model-difference feature there might be an actual realistic reason for this that stems from the difference between opportunistic charging anywhere and home-charging. The Markov chain model limits individuals from too long excursions by requiring home-charging, which can be interpreted as a form of range-anxiety, see [176] for a study on range anxiety using this model. The probability distribution model on the other hand lacks any conceptual connection to range anxiety since the charging stations in that model are considered maximally abundant by the "charging anywhere when stopped" assumption. The electricity use profile from the probability distribution model has a peak in the morning and a larger peak in the evening which differs from the electricity use profile from the Markov chain model which indicates a stark prevalence of charging during evening and nighttime. This suggests different applicability of the models. It should be noted that it is possible to combine these two models to achieve a home-charging probability distribution model, which was realized in Paper (VIII), see Section 3.4.2.

4.4 Grid interaction and self-consumption

This section investigates self-consumption and grid interaction for the combination of PV power production, household electricity use and EV charging with different models. First results from the complete model combining the Widén model and the EV extension with PV power production estimated from solar irradiation are provided in Section 4.4.1. Second, results from the complete probability distribution model combining PV power production, household electricity use and EV charging are presented in Section 4.4.2.

4.4.1 Markov chain electric vehicle charging model

In paper (VII) the correlation between household electricity use and EV home-charging with PV power production was investigated by using the Widén model for household electricity use with EV home-charging extension. The one minute resolution of PV power production for the Ångstrom Laboratory at Uppsala Sweden (59°50′19” N 17°38′50” E) during January 1 to December 31 2011 was used along with the setup of household electricity use and EV charging described in Section 4.3.1. The PV power production was setup with 45 degrees tilt, facing south. The module efficiency was set to 17 percent, and the system efficiency set to 13 percent. See Section 3.2.6 for more information on PV modeling from solar irradiance data.

With this setup the yearly net-zero energy PV power production for the two resident detached house was generated by 25 m^2 PV panels, corresponding to 4.3 kW_p. The yearly net-zero energy setup of the EV charging when using the Markov chain EV model with Tesla Model S setup in Table 4.3 is 30 m^2 PV panels, corresponding to 5.1 kW_p. The total net-zero energy PV area setup is 55 m^2 which then corresponds to 9.4 kW_p. The average daily power production and consumption for each setup is shown in Figure 4.10. On average EV charging increases the load during evening and nighttime and PV power production is centered around noon. Since this is a year average plot over diurnal electricity use it is tempting to estimate matching by inspection. However averages can be misleading, instead the duration of the time series of the generated data should be examined, as is done in Figure 4.11. It should be noted that in paper (VII) the setup was different from the Tesla Model S setup, in particular the available battery capacity was there set to 14 kWh instead of 85 kWh as here. The choice of a large battery capacity for the simulations presented in this results section is to more accurately represent the largest battery capacity available today as an extreme scenario, and also to address future scenarios for EVs, which in all likelihood have larger battery capacities on average compared with today's standards.

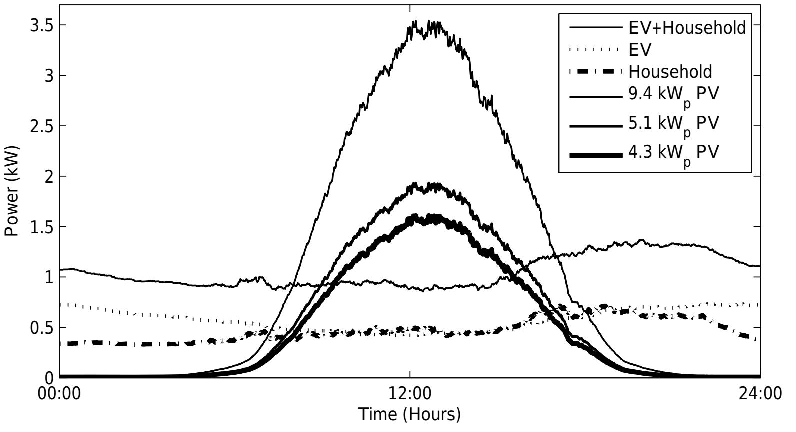

Figure 4.10. Year average daily power production from various net-zero energy setup of PV power production and power consumption from two resident household electricity use and EV home-charging. The PV power production is generated by the linear model based on solar irradiance presented in Section 3.2.6, synthetic household electricity use and EV home-charging are generated from the Markov chain models, see Sections 3.3.1 and 3.4.1.

In order to show grid interaction Figure 4.11 displays a duration diagram for each component and for the combination of components.

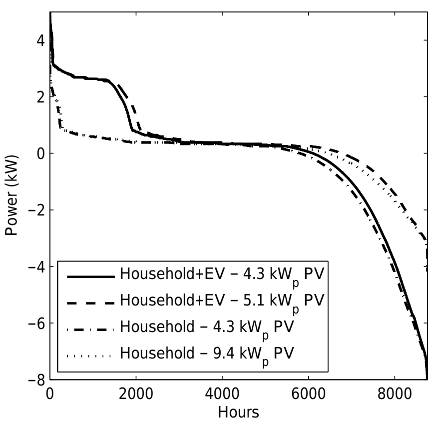

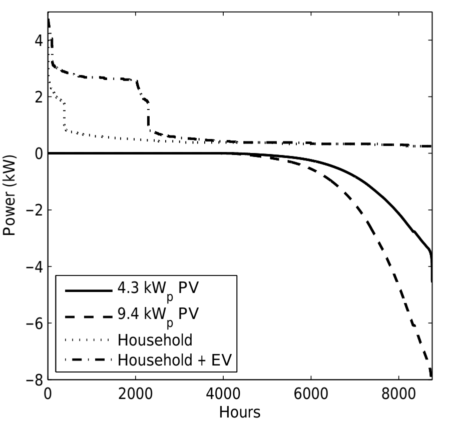

Figure 4.11. Duration plot representing one year electricity use associated with PV power production, household electricity use and EV charging for various combinations. The 9.4 kW$_\text{p}$ PV setup is net-zero energy setup for household + EV whereas 4.3 kW$_\text{p}$ is net-zero energy setup for only household electricity use.

The duration diagrams in Figure 4.11 show that the introduction of EV home-charging increases the high power load, and when the PV power production is added there is a reduction of household and EV charging load, but at the cost of net injection of electricity into the grid.

4.4.2 Probability distribution model

This section presents the results from paper (VIII) regarding the complete probability distribution model which combines the probability distribution models for PV power production, household electricity use and EV home-charging developed in papers (I), (III) and (V). Here household electricity use, EV home-charging and PV power production are labeled as "components" in the probability distribution model.

The study in paper (VIII) was developed according to descriptions in Section 3.6.1. The household electricity use was obtained from the Weibull probability distribution model developed in paper (III) and described in Section 3.3.2. The PV power production was setup as yearly net-zero energy with respect to the household electricity use: 81 m^2 PV system with 42 degrees tilt facing south with efficiency 150 W/m^2 resulting in 12.2 kW_p. EV home-charging was simulated using the EV probability distribution model described in Section 3.4.2, but with probabilities for charging calibrated by the Markov chain EV home-charging model described in Section 3.4.1. The Markov chain EV home-charging model was setup with the parameters in Table 4.6, along with the seasonal seasonal coefficient (see Section 3.4.1).

Table 4.6. *Setup on EV charging in the complete probability distribution model, for nomenclature see Table 3.4.*

p_{EV}	C^{Charge}	C^{PEV}	SOC_{min}	SOC_{max}	D	V	v
0.2	2.3 kW	8.4 kW	21 kWh	35 kWh	37 km	46 km/h	0.2 kWh/km

This was studied on two system levels: individual household level and aggregates of households. Initially the individual household level will be described, followed by aggregate levels of households. Results for one year minute-resolution data can be seen in Figure 4.12.

Probability distribution modeling of each power consuming/producing component at the end-user in the grid gives an indication of the grid interaction. In Figure 4.12 the probability density distribution on the positive side represents a histogram of consumed electricity from the grid, and the part of the probability density distributions on the negative side represents a histogram of electricity injected into the grid. Only the magnitude of the probability density distribution at zero represents self-consumption. When adding standard setup

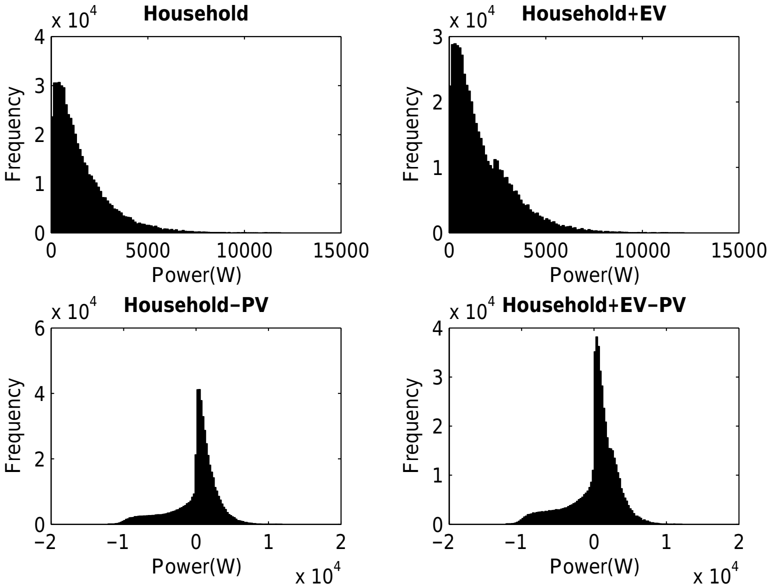

Figure 4.12. Histograms of probability distributions obtained via convolution for each setup of PV power production, household electricity use and EV home-charging generated from models developed in papers (I), (III), (V) and presented in paper (VIII). See Section 3.6.

EV charging to the typical Weibull distribution setup of household power consumption the effect is a small bump at around 2.3 kW. One has to keep in mind that the magnitude in the histogram does not necessarily represent the actual impact on the grid, it only describes the probability for each level of power consumption/production. For this setup the household electricity use is 13.6 MWh/year and the EV charging is about 1.7 MWh/year, and the PV power production is sized to achieve annual net-zero energy consumption with respect to the household electricity use.

The probability density distributions for each configuration of components over time of day for a year using surface plots of histograms is shown in Figure 4.13. In this plot it is possible to see the average diurnal variation in grid interaction, above all the probability distribution of PV power production injected into the grid is prominent, despite being a net-zero energy setup. This highlights the mismatch issue of intermittent PV power production, household electricity use and EV home-charging from a probability distribution perspective.

The self-consumption measures of instantaneous load fractions (3.50) and solar fractions (3.49) become probability density distributions in the probability distribution model. These probability density distributions are shown in the form of histograms produced by the model, shown in Figure 4.14. The

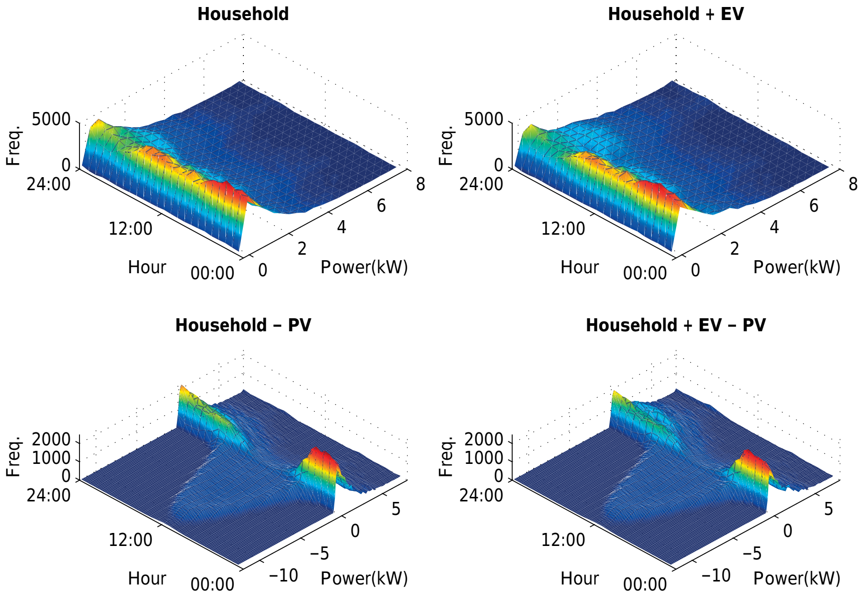

Figure 4.13. Surface plots over daily power consumption/production histograms for each setup in the probability distribution model combining PV power production, household electricity use and EV home-charging generated from models developed (I), (III) and (V) and presented in paper (VIII).

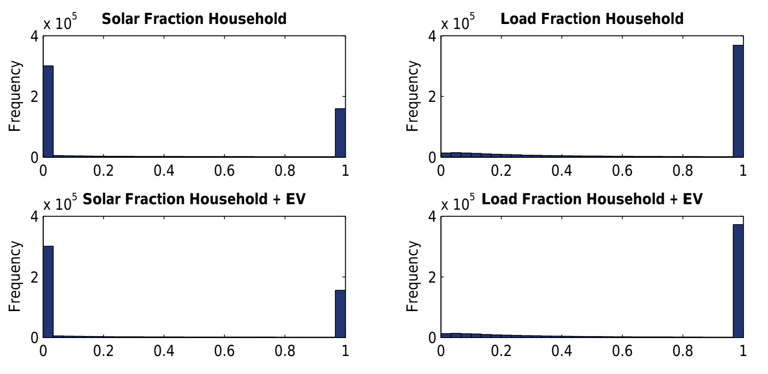

Figure 4.14. Histograms over instantaneous solar fraction and load fraction from the probability distribution model combining household electricity use, EV home-charging and PV power production generated from models models developed (I), (III) and (V) and presented in paper (VIII).

result shows that the solar fraction is approximately Bernoulli distributed, having peaks around zero and one. By the definition of the solar fraction (found in Section 3.6.2) this means that the household electricity use is most of the time either completely covered by PV power production or it is not covered at all. The introduction of the EV does not change this situation, perhaps fast-charging could change the distribution more significantly, which could have an effect on the solar fraction. The load fraction histogram on the other hand hints a descending distribution from zero up to one where there is a peak. The load fraction represents by definition the level of PV power production which is covered by load. The peak at one has an obvious explanation since the model includes nighttime when there is no PV power production, and it is completely covered by load. The reason for the descending Gamma or Weibull type of distribution between zero and one is less obvious to explain, but it is probably related to mornings and evenings and possible winter time since during those occasions there is less PV power production — but not necessarily zero. Also the load fraction does not change in any significant way when the EV is introduced with the setup in this paper.

One has to keep in mind that in this particular probability distribution model there is no dependence between each component as they are considered independent by approximating assumptions. An approach which accounts for this correlation, for example between EV charging and household electricity use, would probably give different results.

These results represent the individual household level. The paper also includes an investigation of the effect of the power consumption/production distributions of aggregates of households.

The histogram line plot for the individual household scenario presented in Figure 4.15 is identical to the histogram in Figure 4.12. As the number of houses increase there are only small changes compared with the original distribution for power consumption and production. Above all the resulting distribution does not appear to converge a Normal distribution, which was the case for the individual probability distribution models of PV power production, household electricity use and EV charging as a result of the central limit theorem. For the combined model there is an indirect dependence between each component, which violates the variable independence criterion of the central limit theorem. Thus despite the fact that the probability distributions are independent variables by onset, they share indirect dependencies such as diurnal and yearly variations in solar irradiance. This artefact arises because the fit-to-distribution process for each model is performed for different time bins, such as seasonal and diurnal time-bins for the household electricity use model, which then connects to the (deterministic) seasonal and diurnal variation of PV power production. This non-Normal distribution feature in the power consumption/production of aggregates of households is interesting because it highlights the dependence between each component of the system. In turn this is interesting from a grid perspective, where aggregates of households are used for design and operation of the local electricity grid.

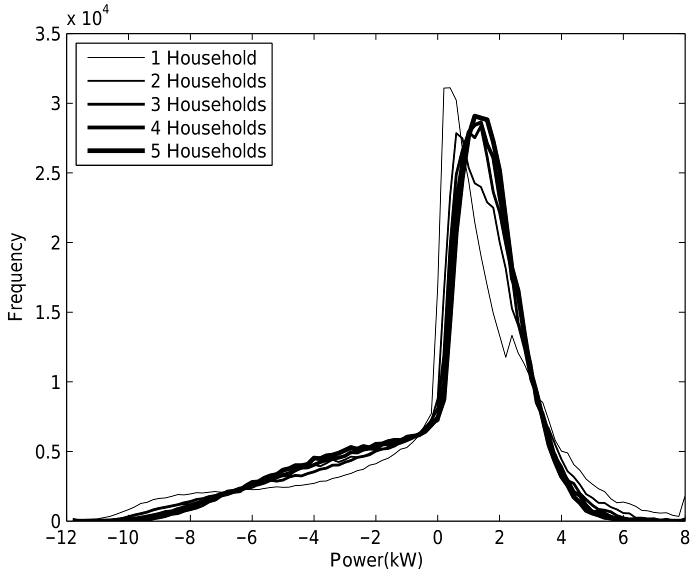

Figure 4.15. A line plot based on a histogram of power consumption for the setup of aggregates of PV power production, household power consumption and EV home-charging generated from the complete probability distribution model developed in (VIII), based on papers (I), (III) and (V). The PV setup is 81 m^2, or 12.2 kW_p for each household, which corresponds to net-zero energy with respect to the household load on a yearly basis.

4.5 Case studies

This section presents case studies regarding PV power production, household electricity use and EV charging. First a study on PV power production, household electricity use and EV charging in the City of Westminster is presented in Section 4.5.1 and then an analysis of PV power production and EV charging from eight solar charging stations is presented in Section 3.5.

4.5.1 City of Westminster case study

In paper (VI) the self-consumption and grid interaction study presented in paper (VII) was applied to a case study of the City of Westminster, London. In that study data for solar irradiance was provided by the software Meteonorm [170]. Data for the City of Westminster was used such as available rooftop area from UKMap [177] and data on number of residents per household [178, 179]. A scenario of maximum introduction of PV in the City of Westminster was identified from UKmap with the assumption that 25% of available rooftop area (due to e.g. chimneys) could be feasible for PV. The Markov chain model for household electricity use and EV home-charging was then used to characterize

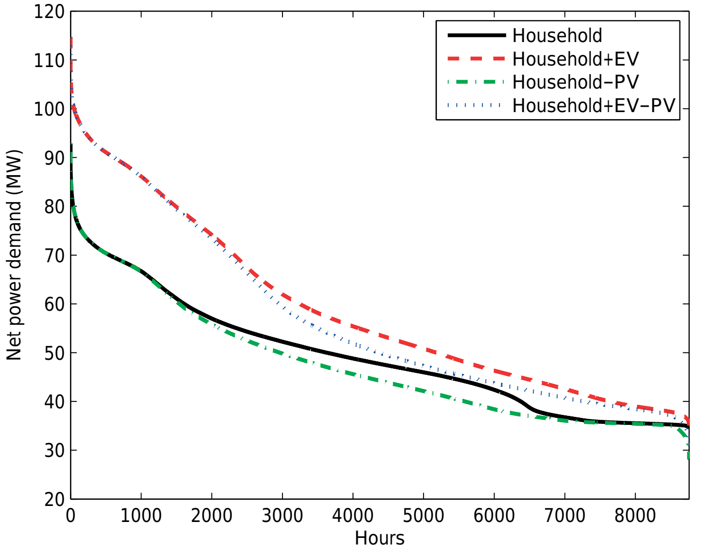

Figure 4.16. A one year duration diagram over the simulated power consumption from household activities and EV home-charging with PV power production in the City of Westminster. The simulation was setup with an assumption of complete electrification of all current vehicles and with a maximum feasible coverage of PV in the City of Westminster.

electricity consumption and production for each household size and for the entire City of Westminster. A duration diagram of the electricity use for the City of Westminster with household electricity use, all 48,810 current vehicles replaced with home-charged standard setup EVs (with setup from Table 4.6) and a maximum coverage of 465,509 m^2 or 70 GW$_p$ PV (assuming 15 percent system efficiency) is shown in Figure 4.16.

The results show that a maximum feasible introduction of PV in the City of Westminster showed no net production of electricity. The total electricity use and standard deviation of electricity use for each scenario is given in Table 4.7.

This table shows the small effect on total electricity use of introducing EV charging and/or PV power production, but with a higher standard deviation of electricity use for those scenarios. This could have an effect on the power grid, in particular at the end-user where the variability is larger.

4.5.2 Solar charging station data

In paper (IX) data for EV charging and PV power production from eight Solelia Greentech solar charging stations distributed across southern Sweden

Table 4.7. *Energy use and standard deviation of power consumption for the different scenarios for the City of Westminster.*

System setup	Energy use (GWh/yr)	Net power demand Std (MW)
Households	431	11.5
Household + EV	514	17.5
Households - PV	416	11.9
Households + EV - PV	498	18.2

was quantified and analyzed. The solar charging stations and the data are described in Section 3.5.

Each solar charging station was based on different charging conditions: free public charging or free charging for the company owning the charging station. The data set was one-minute resolution for 281 and 310 consecutive days of data (depending on station) with a lack of PV power production data for two stations. Data on cumulative EV charging during the periods for each station along with cumulative PV power production for the same stations are given in Table 4.8.

Table 4.8. *Total electricity production and consumption for each solar charging station.*

Station	Dates	Production (kWh)	Consumption (kWh)
1	08Sep2013 - 06Jul2014	0	162
2	08Sep2013 - 06Jul2014	0	342
3	08Sep2013 - 06Jul2014	493	373
4	08Sep2013 - 06Jul2014	493	795
5	08Sep2013 - 14Jul2014	603	214
6	08Sep2013 - 14Jul2014	603	260
7	07Oct2013 - 14Jul2014	544	338
8	07Oct2013 - 14Jul2014	544	744

The cumulative electricity use from EV charging is at a similar level compared with the cumulative PV power production during the same period of time for most solar charging stations. The average diurnal variability of EV charging and PV power production for each solar charging station is shown in Figure 4.17.

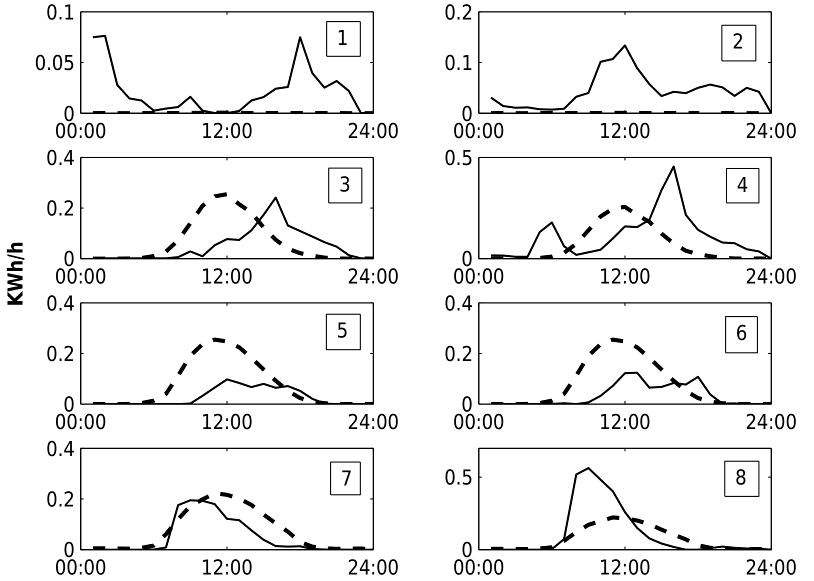

Figure 4.17. Plots representing average daily electricity consumption and production data with hour-resolution from the solar charging stations. From upper left to lower right the plots represent the output from stations 1-8 included in paper (IX). The solid line represents the average daily EV charging power consumption profile and the dashed line the PV power production. Note that in order to highlight the profiles for each station the y-axis limits differs between the plots.

In this figure there is a large variation between the EV charging power profiles in terms of both diurnal variability and average magnitude. These can be compared with the results of the EV charging models developed in papers (V) and (IV), shown in Section 4.3.

The EV charging model developed in paper (V) was based on an opportunistic charging scheme, charging whenever the vehicle stops, while the EV charging model developed in paper (IV) was based on home-charging only. The difference between these approaches compared with the setup of the solar charging stations is that the EV modeling was based on the actions of one EV, and where it was charged, whereas the data was obtained from each charging station, regardless of the number of EVs. This makes a complete comparison impossible. Despite this the diurnal variability of station 1 is somewhat similar to EV home-charging (at least for small battery setup, see paper (IV)) and station 4 is similar to opportunistic EV charging. Any reason for these potential connections is yet to be found.

grid interaction in terms of self-consumption is presented in Table 4.9. The level of self-consumption — in terms of load fraction — varies between 0.2 and 10 percent, and a study by means of the probability distribution models of only EV as a means for PV self-consumption based on models is yet to be done, thus no comparison can be made so far. Nevertheless, there is a large potential for improvement regarding PV self-consumption by means of EV charging. A first step is to maximize the amount of EVs that charge at the solar charging stations, a second step could perhaps be to introduce smart-charging schemes, such as various incentives for charging at different times during the day.

Table 4.9. *Total grid interaction and self-consumption of the solar charging stations.*

Station	Net consumption (kWh)	Net production (kWh)	Self-consumption (kWh)
1	162	0	0
2	342	0	0
3	363	483	10
4	759	457	36
5	592	203	11
6	586	243	17
7	512	306	32
8	506	706	38

5. Discussion

This chapter presents a discussion on the topics and results presented in the thesis and the appended papers.

5.1 Discussion

Gaining insight, by means of devising accurate models with potential forecasting, of the space-time variability of solar irradiance on Earth's surface is of direct use in utilizing renewable energy via PV systems. In combination with models for electricity use from residential houses and potential EV charging this presents interesting possibilities for optimization.

EV charging patterns are highly dependent on conditions for charging. The difference between the Markov chain home-charging model and the probability distribution model for opportunistic charging is highlighted both in magnitude and variability. Also solar charging station data indicates a strong variability between stations, which suggests that EV charging is perhaps more suitably modeled on the basis of stations and their setup rather than on the basis of the EV users.

Generally, probability distribution models present a good way of condensing large sets of data into manageable systems with preserved information regarding variability. When applied to electricity use and production these models present valuable information regarding the magnitude and variability of grid interaction and load matching which can assist in devising grid interaction indicators [35]. The use of probability distributions for characterizing power production and demand on an individual household level also assist in the process of modeling power production and demand from aggregates of households via methodologies of probability distribution theory. This has applications for grid calculations and can assist in power system design and policy development. It can also assist in the analysis of for example NZEB electricity consumption and production mismatch.

5.2 Future work

This thesis provides models and research regarding PV power production, household electricity use, EV charging and the combinations thereof. There is more to be done within these topics. I hope the following comes to fruition.

The combination of PV power production and only EV charging, both home-charging and charging elsewhere is interesting to quantify. Also since real-life data on EV charging is scarce it would be interesting to continue the analysis of model predictions in this thesis compared with actual data on EV charging. This could also prove to be a useful pursuit in attempts to sort out relevant models in the massive — and expanding — body of literature on EV charging models.

A continued study of PV power production, household electricity use and EV charging in terms of probability distributions could prove interesting for estimating grid interaction. In turn this could be used in advanced calculations for estimating grid-impact.

Studies on forecasting PV power production with probability distribution modeling could be interesting, in particular for the setup of smart-home management systems. Generally pushing the state-of-the-art of solar irradiance modeling for single and multiple locations is of importance for PV power production estimates globally.

The development and direct utilization of approximating statistical methods could dramatically improve the applicability of statistical models for PV power production, household electricity use and EV charging.

Also implementing easy-to-use smart charging strategies for EVs could be interesting to investigate both theoretically via modeling, but also via real-life implementations. This is particularly interesting in connection with PV power production, such as for the solar charging stations.

Generally devising test studies for implementation of PV systems and EV charging stations for houses and neighborhoods presents a great opportunity to verify models and to identify new research opportunities while simultaneously providing residents with state-of-the-art energy efficient technology.

6. Summary of conclusions

This chapter summarizes the main conclusions of the studies presented in this thesis. This relates to the aims presented in Section 1.1 and identified research gaps in Section 2.6.

Solar irradiance and PV power production modeling (Papers (I)-(II))

- It was shown that a stochastic variable with a bimodal Normal mixture distribution could be used to model the clear-sky index, subsequent solar irradiance and PV power production. For remote locations the aggregate clear-sky index was shown to approach a Normal distribution.

- With the aid of Gamma-distributed and Bernoulli-distributed stochastic variables it was possible to show a correlation between solar irradiance and number of bright sunshine hours over time by providing a generalized Ångström equation.

Household electricity use modeling (Paper (III))

- It was shown that it is possible to model household electricity use with either Weibull or Log-normal distributed stochastic variables. For aggregates of households the resulting electricity use profile at any moment was shown to approach a normal distribution as the number of households increased.

Electric vehicle charging modeling (Papers (IV)-(V))

- EV home-charging was modeled as an extension to the Widén Markov chain model for generating synthetic household electricity use patterns. EV home-charging was shown to have a peak during evening and night time with a yearly electricity use of 1.6-5.6 MWh/year.

- It was shown that EV charging could be modeled via Bernoulli distributed stochastic variables. For aggregates of EVs the probability distribution for charging was shown to approach a normal distribution.

Modeling of PV power production, household electricity use and EV charging (Papers (VI)-(VIII))

- A complete model of PV power production, household electricity use and EV charging was developed using stochastic variables. Indirect dependencies between each component of the model implied that the resulting power consumption/production was not normally distributed for aggregates of households with this model (in contrast to the results of the individual components).

- A complete model of PV power production, household electricity use and EV charging with the use of data on solar PV power production and Markov chain models of household electricity use with EV home-charging was developed. Results from simulations indicated that while the EV increases the self-consumption of PV power production it increases the total electricity use from the grid due to evening and night-time charging.

- As a case study for the City of Westminster a complete model of PV power production, household electricity use and EV charging was developed. The model was based on the Widén Markov chain model for household electricity use and with EV home-charging extension combined with PV power production obtained from a PV model and Meteonorm data. In no feasible scenario did PV power production exceed the power consumption of the households in the city.

Analysis of EV charging and PV power production from solar charging stations (Paper (IX))

- Data on EV charging and PV power production from eight Solelia Greentech AB solar charging stations was quantified and analyzed. The charging patterns of the solar charging stations were shown to be diverse in magnitude and diurnal as well as seasonal variability. The cumulative electricity use of EV charging covered PV power production between 43% and 162% for the duration of the study, but due to mismatch between power consumption and production the PV self-consumption (Load fraction) was between 0.2% and 10%.

7. Sammanfattning på svenska

Genom sjunkande priser på solceller så har solelinstallationer, speciellt på hustak hos privatpersoner, blivit allt vanligare i Sverige och världen över. Nästan alla installationer är idag dessutom inkopplade direkt till elnätet vilket gör att man kan leverera den del av solelen som man själv inte konsumerar till elnätet. Beroende på lagar och avtal för leverans av solel till nätet så kan man tjäna på att antingen sälja den egenproducerade elen till nätet eller att använda den själv genom hushållselanvändning eller exempelvis elbilsladdning. Det är därför intressant att undersöka hur solelproduktionen sammanfaller med elkonsumptionen.

Hur väl solelproduktion överensstämmer med hushållselanvändning är till viss del känd sedan tidigare, men hur väl den stämmer överens med elbilsladdning har varit en öppen frågeställning. Genom stigande priser på bensin och diesel samtidigt som batterier och elbilstekniker förbättrats så har det blivit allt mer lönsamt och vanligare med elbilar och hybrider, det vill säga elbilar med en extramotor som går på bensin eller diesel. Det har även blivit allt vanligare att hybrider går att ladda direkt från elnätet med plug-in teknik. Eftersom både nätansluten solel och elbilsladdning utgör en belastning på elnätet så är det önskvärt att undersöka detta från ett elnätperspektiv, speciellt inför framtida elnätsförbättringar.

I denna avhandling så presenterar jag forskning kring solelproduktion, användning av husehållsel samt elbilsladdning. Jag har skapat matematiska modeller som återspeglar verklig solelproduktion, hushållselanvändning och elbilsladdning för individuella hushåll, för grupper av hushåll samt för hela städer. Dessa modeller är utvecklade utifrån principer och antaganden samt uppmätta data som relaterar till solel, hushållsel och elbilsladdning och utgör en del av resultatet av denna avhandling. Modellerna, samt analys av data för solelproduktion och elbilsladdning, vilka presenteras i denna avhandling, är publicerade i internationellt ansedda vetenskapliga tidsskrifter.

Resultaten visar att elbilsladdning hemma troligen mestadels kommer att ske under sen eftermiddag, kvällstid och natt. Tillsammans med solel och hushållselkonsumtion så visar detta att elbilsladdning ökar egenanvändningen av solel, men att elbilsladdning hemma till största delen inte laddas med solel utan från nätet, oavsett storlek på solcellsystemet. En annan modell för elbilsladdning utvecklades där elbilen laddades varje gång den stannade. Denna modell visade på elbilsladdning under middag och eftermiddag, något som kan visa sig vara mer effektivt för matchning mot solelproduktion. En av studierna som är inkluderade i avhandlingen är en fallstudie av stadsdelen Westminster i London, Storbritannien, som genomfördes tillsammans med forskargruppen EECi vid universitetet i Cambridge. Där konstaterades att solelproduktionen från en komplett rimlig beläggning av solceller i stadsdelen inte skulle överstiga elkonsumptionen från hushållen. I en annan studie gjordes en analys av uppmätt elbilsladdning och solelproduktion för åtta av Solelia Greentech ABs solcellsladdstationer.

De modeller jag har utvecklat har även använts i elnätsstudier som utförts tillsammans med STRI och Sweco för att uppskatta nödvändigheten för förbättringar av Svenska elnätet framöver. Vidare forskning inriktas på att fortsätta undersöka solelproduktion, hushållselkonsumtion och elbilsladdning från olika perspektiv samt att utveckla mer avancerade matematiska modeller.

8. Acknowledgements

This work has been carried out within the Built Environment Energy Systems Group, Division of Solid State Physics, Department of Engineering Sciences at Uppsala University. The project was primarily financed by the Energy Systems Programme, which is financed by the Swedish Energy Agency. Funding was also provided by the Swedish Energy Agency programs: "Demonstration projects for efficient use of locally produced solar electricity for electric vehicles" and "Increased consumer power in the Nordic electricity market". Funding for travel and accommodation for the external research project at the University of Cambridge was provided by Håkanssons travel grant. I would like to take the opportunity to thank Ångström Academy for awarding me the Ångström Innovation prize and scholarship 2014.

This thesis was made possible with the support of a number of people. First off I would like to thank my main supervisor Dr. Joakim Widén for his excellent supervision and scientific guidance throughout the duration of my time as a PhD-student. My co-supervisor Dr. Ewa Wäckelgård for her support and for providing insight into the infrastructure of power systems research. My second co-supervisor Dr. Jesper Rydén for supercharging my stochastic models to a state-of-the-art level. Also my previous co-supervisor Dr. Kajsa Ellegård for providing me with valuable socio-technical insights.

The members of the Program Energy Systems who set the stage for interesting collaborations, courses and research debates, in particular Dr. Pia Grahn and Mattias Hellgren for collaborations on courses and research. Also my co-authors Dr. Karin Alvehag and Dr. Lennart Söder from KTH.

A special thanks goes to Dr. Ruchi Choudhary, Dr. Juan-José Sarralde, Dr. Wei Tian and Dr. Justin D. K. Bishop at EECi at the University of Cambridge for collaboration on the Westminster-project, and for their hospitality during my research visits.

Also Per Wickman at Solelia Greentech AB for providing an interesting opportunity to work with actual PV power production and EV charging data. Furthermore I thank Dr. Katarina Yuen Larsson and Mårten Larsson at Sweco as well as Susanne Ackeby at STRI for collaborations which made it possible to use our electric vehicle charging models into applied Swedish power system case studies via Elforsk.

Thanks goes to Dr. Clas-Göran Granqvist, Dr. Peter Svedlindh and to the Division of Solid State Physics at Uppsala University. The Built Environment Energy Systems Group (BEESG) members: Dr. Magnus Åberg, Dr. Annica Nilsson, David Lingfors and Rasmus Luthander. All of my colleagues at the division of solid state physics for providing a social and hospitable atmosphere, in particular Bengt Götesson for presenting valuable high-tech suggestions.

Thanks also goes to Dr. Fredrik Wallin and Javier Campillo at Mälardalens Högskola (MdH) for research collaborations. Dr. Uwe Zimmerman for providing highly resolved solar irradiance data from the very PV panels I watch every day outside the window of my office. My office mate and business partner Yajun Wei for interesting discussions and excellent cooperation. Dr. Lars Mattsson at Nordita for providing me with extremely challenging — but fun — astrophysical mathematical problems whose solutions, as it turns out, has applications even in power systems research.

I would like to thank my wife Anna Munkhammar for her joyful attitude and strong forcing for directions such as heavy running and enjoying life. I thank my family and friends for putting life in a meaningful context. Special thanks to my parents and my brother Johnny Munkhammar (1974-2012), whom without this achievement would never have been made.

References

[1] Madison, A., The World Economy: A Millennial Perspective, OECD, Paris 2001.
[2] Intergovernmental Panel on Climate Change, Renewable Energy Sources and Climate Change Mitigation, Cambridge University Press New York 2012.
[3] Molin, A., Rohdin, P., Moshfegh, B., Positive power market value for grid-connected roof-top solar power in Sweden, in proceedings World Renewable Energy Congress September 2010, Abu Dhabi, UAE.
[4] The Swedish Energy Agency, Solar Power and Solar Synthesis Report: Technology market and research activities 2006-2011, ER 2012:17, 2012.
[5] Widén, J., System Studies and Simulations of Distributed Photovoltaics in Sweden, Dissertation Uppsala University, 2010.
[6] United States Department of Energy, Smart Grid, `http://energy.gov/oe/services/technology-development/smart-grid` (Retrieved 2015-01-21).
[7] Bollen, M. H. J., Hassan, F., Integration of Distributed Generation in the Power System, Wiley IEEE press series on Power Engineering, 2011.
[8] Walla, T., Widén, J., Johansson, J., Bergerland, C., Determining and Increasing the Hosting Capacity for Photovoltaics in Swedish Distribution Grids, ín proceedings of 27th European PV Solar Energy Conference (EU-PVSEC), Frankfurt 2012.
[9] Widén, J., Nilsson, A. M., Wäckelgård, E., A combined Markov-chain and bottom-up approach to modelling of domestic lighting demand, Energy and Buildings 2009: 41; 1001-1012.
[10] Widén, J., Wäckelgård, E., A high-resolution stochastic model of domestic activity patterns and electricity demand, Applied Energy, 2010: 41; 1880-1892.
[11] Bertalanffy, L., General Systems Theory, George Braziller, New York 1968.
[12] Gustafsson, L. G., Lanshammar, H., Sandblad, B. L., System och Modell: En introduktion till systemanalysen, Studentlitteratur (1982).
[13] Dyson, F. J., Search for Artificial Stellar Sources of Infra-Red Radiation,. Science 1960: 131 (3414); 1667-1668.
[14] Munkhammar, J., Tankar från en principfast pragmatiker, Timbro förlag, Stockholm 2014.
[15] Schavemaker, P., van der Sluis, L., Electrical power system essentials, Wiley, Chichester 2008.
[16] Högselius, P., Kaijser, A., När folkhemselen blev internationell. Elavregleringen i historiskt perspektiv, SNS publisher 2007.
[17] The Swedish Energy Agency, Vindkraftstatistik 2013, ES2014:02, 2014.
[18] Lindahl, J., Svensk sammanfattning av IEA-PVPS National Survey Report of PV power applications in Sweden 2013, Report Swedish Energy Agency 2013.
[19] Svensk Energi, Svenska elnätet, `http://www.svenskenergi.se/Elfakta/Elnatet/` (2015-01-08).

[20] Svenska kraftnät, Kort om Svenska kraftnät, Fact sheet 2014.
[21] REN21, Renewables 2014 Global Status Report, Paris: REN21 secretariat 2014.
[22] Encyclopedia Britannica, Renewable Energy, accessed online at `http://global.britannica.com/EBchecked/topic/17668/renewable-energy` (2015-01-07).
[23] International Energy Agency, Trends in photovoltaic applications: Survey report of selected IEA countries between 1992 and 2012, Report IEA-PVPS T1-23:2013, 2013.
[24] EPIA, Global Market Outlook for Photovoltaics 2014-2018, Report 2014.
[25] Green, M. A., Solar Cells, Prentice-Hall series in solid state physical electronics 1981.
[26] Fraunhofer Institute for Solar Energy Systems, Photovoltaics Report, Freiburg 2014.
[27] Civicsolar, Yingli Solar YL 240 P-29b 240W Poly SLV/WHT Solar Panel, `http://www.civicsolar.com/product/yingli-solar-yl-240-p-29b-240w-poly-slvwht-solar-panel`, (Retrieved 2015-01-08).
[28] Widén, J., Wäckelgård, E., Lund, P. D., Options for improving the load matching capability of distributed photovoltaics: Methodology and application to high-latitude data, Solar Energy 2009: 83; 1953-1966.
[29] SunEdison, Enabling the european consumer to generate power for self-consumption, SunEdison Report 2011.
[30] IPVEA , Super charged: self-consumption sparks alliances between PV and storage industries, Energy storage journal 1, 2012.
[31] Beister, D., Sophisticated Energy Management for Optimizing the PV Grid Interaction, In conference Proceedings of the 27th European Photovoltaic Solar Energy Conference and Exhibition in Hamburg 24-28 September, Germany, 2012; 4101 - 4104.
[32] SMA, Sunny home manager, `http://www.sma.de/en/products/monitoring-control/sunny-home-manager.html`, (Retrieved 2015-01-08).
[33] Braun, M., Büdenbender, K., B., Magnor, D., Jossen, A., Photovoltaic Self-Consumption in Germany - Using Lithium-ion Storage to Increas Self-Consumed Photovoltaic Energy, in proceedings of 24th European Photovoltaic Solar Energy Conference, 21-25 September, Frankfurt Germany, 2009; 3121-3127.
[34] Castillo-Cagigal, M., Caamaño-Martín, E., Gutiérrez, A., Masa-Bote, D., Monasterio-Huelin, F., Porro, F., Matallanas, E., Jiménez-Leube, J., Self-Consumption of PV Electricity with Active Demand Side Management: The GeDELOS-PV System, in proceedings of the 25th European Photovoltaic Solar Energy Conference and Exhibition 6-10 September in Valencia, Spain, 2010; 4866-4870.
[35] Salom, J., Marsal, J. A., Widén, J., Cardanedo, J., Lindberg, K. B., Analysis of load match and grid interaction indicators in net zero energy buildings with simulated and monitored data, Applied Energy 2014: 136; 119-131.
[36] Fattori, F., Anglani, N., Muliere, G., Combining photovoltaic energy with electric vehicles, smart charging and vehicle-to-grid, Solar Energy 2014: 110;

438-451.
[37] Luthander, R., Widén, J., Nilsson, D., Palm, J., Photovoltaic self-consumption in buildings: A review, Applied Energy 2015: 142; 80-94.
[38] Ångström, A., Note on the relation between time of sun shine and cludiness in Stockholm 1908-1920, Arkiv för matematik, astronomi och fysik, kungliga vetenskapsakademien, 1922: 17; 1-7.
[39] Ångström, A., Solar and terrestrial radiation, Q. J. Roy. Met. Soc. 1924: 50; 121-126.
[40] Ångström, A., On the computation of global radiation from records of sunshine, Arkiv fur Geofisik 1956: 5; 41-49.
[41] Black, J. N., Bonython, C. W., Prescott, J. A., Solar Radiation and the duration of sunshine. Q. J. Roy. Met. Soc. 1954: 80; 231-235.
[42] Glover, J., McCulloch, J. S. G., The empirical relation between solar radiation and hours of sunshine, Q. J. Roy. Met. Soc. 1958: 84; 172-175.
[43] Bennet, I., Frequency of daily insolation in Anglo North America during June and December, Solar Energy 1967: 11; 41-55.
[44] Klein, S. A., Calculation of monthly average insolation on tilted surfaces, Solar Energy 1977: 19; 325-329.
[45] Andretta, A., Bartoli, B., Coluzzi, B., Cuomo, V., Francesca, M., Serio, C., Global solar radiation estimation from relative sunshine hours in Italy, Journal of Applied Meteorology 1982: 21; 1377-1384.
[46] Barbaro, S., Cannata, G., Coppolino, S., Montly reference distribution of daily relative sunshine values, Solar Energy 1983: 31; 63-67.
[47] Liu, B. Y. H., Jordan, R. C., The interrelationship and the characteristics distribution of direct, diffuse and total solar radiation, Solar Energy 1960: 4; 1-19.
[48] Bendt, P., Collares-Pereira, M., Rabi, A., The frequency distribution of daily insolation values, Solar Energy 1981: 27; 1-5.
[49] Hollands, K. G. T., Huget, R. G., A probability density function for the clearness index, with applications, Solar Energy 1983: 30; 195-209.
[50] Saunier, G. Y., Reddy, T. A., Kumar, S., A monthly probability distribution function of daily global irradiation values appropriate for both tropical and temperate locations, Solar Energy 1987: 38, 169-177.
[51] Suehrcke, H., McCormick, P. G., The frequency distribution of instantaneous insolation values, Solar Energy, 1988: 40; 413-422.
[52] Suehrcke, H., The effect of time errors on the accuracy of solar radiation measurements, Solar Energy 1994: 53, 353-357.
[53] Jurado, M., Caridad, J. M., Ruiz, V., Statistical distribution of the clearness index with radiation data integrated over five minute intervals, Solar Energy 1995: 55; 469-473.
[54] Tovar, J., Olmo, F. J., Alados-Arboledas, L., One-minute global irradiance probability distributions conditioned to the optical air mass, Solar Energy 1998: 62; 387-393.
[55] Hollands, K. G. T., Suehrcke, H., A three-state model for the probability distribution of instantaneous solar radiation, with applications, Solar Energy 2013: 96; 103-112.
[56] Ibáñez, M., Rosell, J. I., Beckman, W. A., A bi-variable probability density

function for the daily clearness index, Solar Energy 2003: 75; 73-80.
[57] Assunção, H. F., Escobedo, J. F., Oliviera, A. P., Modelling frequency distributions of 5 minute-averaged solar radiation indexes using Beta probability functions, Theoretical and Applied Climatology 2003: 75; 213-224.
[58] Assunção, H. F., Escobedo, J. F., Oliviera, A. P., A new algorithm to estimate sky condition based on 5 minutes-averaged values of clearness index and relative optical air mass, Theoretical and Applied Climatology 2007: 90; 235-248.
[59] Swedish Energy Agency, Energiläget 2014, Fact sheet 2014, `http://www.energimyndigheten.se/Press/Nyheter/En-samlad-bild-over-energilaget-i-Sverige/` (Retrieved 2015-01-28).
[60] Swan, L. G., Ugursal, V. I., Modeling of end-use energy consumption in the residential sector: A review of modeling techniques, Renewable and Sustainable Energy Reviews 2009; 13: 1819-1835.
[61] Widén, J., Molin, A., Ellegård, K., Models of domestic occupancy, activities and energy use based on time-use data: deterministic and stochastic approaches with application to various building-related simulations, Journal of Building Performance Simulation 2012: 5; 27-44.
[62] McLoughlin, F., Duffy, A., Conlon, M., Characterising Domestic Electricity Consumption Patterns by Dwelling and Occupant Socioeconomic Variables: An Irish Case Study, Energy and Buildings 2012; 48: 240-248.
[63] Widén, J., Lundh, M., Vassileva, I., Dahlquist, E., Ellegård, K., Wäckelgård, E., Constructing load profiles for household electricity and hot water from time-use data — Modelling approach and validation, Energy and Buildings 2009: 41; 753-768.
[64] van Ruijven, B. J., van Vuuren, D. P. , de Vries, B. J. M., Isaac, M., van der Sluijs, J. P. , Lucas, P. L., Balachandra, P., Model projections for household energy use in India, Energy Policy 2011: 39; 7747-7761.
[65] Capasso, A., Grattieri, W., Lamedica, R., Prudenzi, A., A bottom-up approach to residential load modeling, IEEE Transactions on Power Systems 1994; 9: 957-964.
[66] Paatero, J. V., Lund, P. D., A model for generating household load profiles, International Journal of Energy Research 2006: 30;273-290.
[67] Richardson, I., Thomson, M., Infeld, D., A high-resolution domestic building occupancy model for energy demand simulations, Energy and buildings 2008: 40; 1560-1566.
[68] Richardson, I., Thomson, M., Infeld, D., Delahunty, A., Domestic lighting: A high-resolution energy demand model, Energy and Buildings 2009: 41; 781-789.
[69] Walker, C. F., Pokoski, J. L., Residential load shape modeling based on customer behavior, IEEE Transactions on Power Apparatus and Systems 1985; 104: 1703-1711.
[70] Widén, J., Munkhammar, J., Evaluating the benefits of a solar home energy management system: Impacts on photovoltaic power production value and grid interaction, in proceedings of the ECEEE 2013 Summer Study, Presqu'île de Giens, France, June 3-8, 2013.
[71] Ellegård, K., Palm, J.,Visualizing energy consumption activities as a tool for making everyday life more sustainable, Applied Energy 2011: 88; 1920-1926.
[72] Ellegård, K., A time-geographical approach to the study of everyday life of

individuals — a challenge of complexity, GeoJournal 1999: 48; 167-175.
[73] Ellegård, K., Wäckelgård, E., Energianvändning i bebyggelse - boendes och aktörers val av teknik, Universitetstryckeriet Uppsala Universitet 2007.
[74] Zimmermann, J. P., End-use metering campaign in 400 households in Sweden: Assessment of the potential electricity savings, Report Swedish Energy Agency 2009.
[75] Cinlar, E., Introduction to Stochastic Processes, Prentice-Hall International 1975.
[76] Gonzales-Longatt, F., Rueda, J., Erlich, I., Villa, W., Bogdanov, D., Mean Variance Mapping Optimization for the Identification of Gaussian Mixture Model: Test Case, Intelligent Systems (IS), 6:th IEEE International Conference on Intelligent Systeme 6-8 September in Sofia 2012; 158-163.
[77] Herman, R., Kritzinger, J. J., The statistical description of grouped domestic electrical load currents, Electric Power Systems Research 1993; 27: 43-48.
[78] Heunis, S. W., Herman, R., A probabilistic model for residential consumer loads, IEEE Transactions on Power Systems 2002; 17: 621-625.
[79] Irwin, G. W., Monteith, W., Beattie, W. C., Statistical electricity demand modelling from consumer billing data, IEEE Generation, Transmission and Distribution, IEEE Proceedings C 1986; 133: 328-335.
[80] Lin, H-H., Chen, K-H., Wang, R-T., A multivariate exponential shared-load model, IEEE Transactions on Reliability 1993; 42: 165-171.
[81] McQueen, D. H. O., Hyland, P. R., Watson, S. R., Monte Carlo Simulation of Residential Electricity Demand for Forecasting Maximum Demand on Distribution Networks, IEEE Transactions on Power Systems 2004; 19: 1685-1689.
[82] Seppälä, A., Statistical distribution of customer load profiles, in Proceedings of the International Conference on Energy Management and Power Delivery 1995; 2: 696-701.
[83] McLoughlin, F., Duffy, A., Conlon, M., A clustering approach to domestic electricity load profile characterisation using smart metering data, Applied energy 2015: 141; 190-199.
[84] Singh, R., Pal, B. C., Jabr, R. A., Statistical representation of distribution system loads using Gaussian mixture model, IEEE Transactions on Power Systems 2010; 25: 29-37.
[85] Ehsani, M., Gai, U., Amadi, A., Modern Electric, Hybrid Electric, and Fuel Cell Vehicles, CRC Press Boca Raton 2010.
[86] Morea, S. F., The Lunar Roving Vehicle - Historical Perspective, The Second Conference on Lunar Bases and Space Activities of the 21st Century, NASA 1992: 1; 619-632.
[87] Eberle, U., von Helmold, R., Sustainable transportation based on electric vehicle concepts: a brief overview, Energy Environ. Sci., 2010: 3; 689-699.
[88] Tesla Motors, Tesla Model S, `www.teslamotors.com`, (Retrieved 2015-01-08).
[89] Renault S. A., Twizy, `http://www.renault.se/bilar/elbilar/twizy/twizy/`, (Retrieved 2015-01-08).
[90] Nissan Motors Company Ltd, Nissan Leaf, `http://www.nissan.se/SE/sv/vehicle/electric-vehicles/leaf.html`, (Retrieved 2015-01-08).

[91] Cobb, J., Plug-In Car Sales Cross Global Half-Million Mark,
http://www.hybridcars.com/plug-in-car-sales-cross-global-half-million-mark/, 2014 (Retrieved 2015-01-12).
[92] Toyota Europe News Worldwide Prius sales top 3-million mark; Prius family sales at 3.4 million, Green Car Congress,
http://www.greencarcongress.com/2013/ 07/prius-20130703.html, 2013, (Retrieved 2015-01-15)
[93] McLaren Racing Limited, McLaren P1,
http://cars.mclaren.com/home/models_link/McLAREN%20P1/introduction.html, (Retrieved 2015-01-08).
[94] Porche AG, http://904.porsche.com/microsite/918/international.aspx?ws=1, (Retrieved 2015-01-08).
[95] Ferrari S.p.A, http://auto.ferrari.com/en_EN/sports-cars-models/car-range/laferrari/, (Retrieved 2015-01-08).
[96] NLV, NLV Quant, http://www.nanoflowcell.com/quant, (Retrieved 2015-01-08).
[97] Segway inc., Segway PT, http://www.segway.com/, (Retrieved 2015-01-08).
[98] Cobb, J., Top 6 Plug-In Vehicle Adopting Countries.
http://www.hybridcars.com/top-6-plug-in-car-adopting-countries/ 2014 (Retrieved 2015-01-08).
[99] Shahan, Z., Electric vehicle market share in 19 countries,
http://www.abb-conversations.com/2014/03/electric-vehicle-market-share-in-19-countries/ , 2013 (Retrieved 2014-01-08).
[100] Statistics Sweden, Fordonsbestånd 2013, Report 2014.
[101] Larsson, Ö., Ladda för nya marknader: Elbilens konsekvenser för elnät, elproduktion och servicestrukturer, VINNOVA Analys VA 2010:01, 2010.
[102] Dinger, A., Martin, R., Mosquet, X., Rizoulis, D., Russo, M., Sticher, G., Batteries for electric cars - challenges, opportunities and the outlook to 2020, Technical Report the Boston Consulting Group 2010.
[103] Thackaray, M. M. , Wolverton, C., Isaacs, E. D., Electrical energy storage for transportation — approaching the limits of, and going beyond, lithium-ion batteries, Energy & Environmental Sciences 2012: 5; 7854-7863.
[104] Husain, I., Electric and hybrid vehicles: Design fundamentals, second edition, CRC press, Boca Raton 2011.
[105] Marano, V., Onori, S., Guezennec, Y., Rizzoni, G., Madella, N., Lithium-ion batteries life estimation for plug-in hybrid electric vehicles, in proceedings of IEEE Vehicle Power and Propulsion Conference (VPPC), 7-10 September 2009; 536 - 543.
[106] CHAdeMO Association, www.chademo.com, (Retrieved 2015-01-08).
[107] Nissan Motor Company Ltd, Nissan Introduces Quick EV Charger,
http://www.nissan-global.com/EN/NEWS/2010/_STORY/100521-01-e.html, 2010 (Retrieved 2015-01-08).
[108] Laddbil, Laddningstekniker,
http://laddbil.se/ladda-bilen/laddningstekniker/, (Retrieved 2015-01-08).
[109] Tesla Motors, Supercharger,

http://www.teslamotors.com/supercharger, (Retrieved 2015-01-08).
[110] Kutkut, N. H., Divan, D. M. , Novotny, D. W., Marion, R. H., Design Considerations and Topology Selection for a 120-kW IGBT Converter for EV Fast Charging, IEEE Transactions on power electronics 1998: 13; 169-178.
[111] Yongqiang, L., Fuhui, H., Ruilin, X., Tao, C., Jie, L., Investigation on the construction mode of the charging station and battery-exchange station, in proceedings of Asia-Pacific Power and Energy Engineering Conference (APPEEC) 25-28 March in Wuhan, 2011.
[112] Kempton, W., Letendre, S. E., Electric vehicles as a new power source for electric utilities, Transportation Research Part D.: 1997: 2; 157-175.
[113] Habib, S., Kamran, M., Rashid, U., Impact analysis of vehicle-to-grid technology and charging strategies of electric vehicles on distribution networks - A review, Journal of Power Sources 2015: 277; 206-214.
[114] ElNozahy, M. S., Salama, M. M. A., Studying the feasibility of charging plug-in hybrid electric vehicles using photovoltaic electricity in residential distribution systems, Electric Power Systems Research 2014;110; 133-143.
[115] Rajakaruna, S.,Shahia, F., Ghosh, A., Plug In Electric Vehicles in Smart Grid, Springer Power Systems 2015.
[116] Steen, D., Modelling of Demand Response in Distribution Systems, Doctoral Thesis Chalmers University of Technology, Gothenburg, Sweden 2014.
[117] Grahn, P., Electric Vehicle Charging Modeling, Doctoral thesis in electrical systems at the Royal Institute of Technology, Stockholm Sweden 2014.
[118] Ma, Z., Callaway, D. S., Hiskens, I. A., Decentralized Charging Control of Large Populations of Plug-in Electric Vehicles, IEEE Transactions on control systems technology 2013; 21:67-78.
[119] Lindgren, J., Niemi, R., Lund, P. D., Effectiveness of smart charging of electric vehicles under power limitations, International Journal of Energy Research 2014: 38; 404-414.
[120] Lu, L., Han, X., Li, J., Hua, J., Ouyang, M., A review on the key issues for lithium-ion battery management in electric vehicles, Journal of Power Sources 2013; 226: 272-288.
[121] Tie, F. T., Tan, C. W., A review of energy sources and energy management system in electric vehicles, Renewable Sustainable Energy Reviews 2013: 20; 82-102.
[122] Hou, C., Xu L., Wang, H., Ouyang, M., Peng, H., Energy management of plug-in hybrid electric vehicles with unknown trip length, Journal of the Franklin Institute 2014; 115: 174-189.
[123] Richardson, D. B., Electric vehicles and the electricity grid: A review of modeling approaches, Impacts, and renewable energy integration, Renewable and Sustainable Energy Reviews 2013; 19: 247-254.
[124] Torres, J. L., Gonzales, R., Gimenez, A., Lopez, J., Energy management strategy for plug-in hybrid electric vehicles. A Comparative study, Applied Energy 2014; 113:816-824.
[125] Babei, S., Steen, D., Tuan, L., Carlsson, O., Bertling, L., Effects of Plyg-in Electric Vehicles on Distribution Systems: The Real Case of Gothenburg, in proceedings of IEEE PEX Conference on Innovative Smart Grid Technologies Europe 10-13 October in Gothenberg, Sweden, 2010.

[126] Steen, D., Tuan, L. A., Carlsson, O., Bertling, L., Assessment of Electric Vehicle Charging Scenarios Based on Demographical Data, IEEE Transactions on Smart Grid 2012: 3; 1457 - 1468.
[127] Giannuli, M., Yianoulis, P., Study on the incorporation of photovoltaic systems as an auxillary power source for hybtid and electric vechicles, Solar Energy 2012; 86:441-451.
[128] Denholm, P., Kuss, M., Margolis, R. M., Co-benefits of large scale plug-in hybrid electric vehicle and solar PV deployment, Journal of Power Sources 2013; 236: 350-356.
[129] Zhao, J., Kucuksari, S., Mazhari, E., Son, Y.-J., Integrated analysis of high-penetration PV and PHEV with energy storage and demand response, Applied Energy 2013; 112: 35-51.
[130] Dallinger, D., Gerda, S., Wietschel, M., Integration of intermittent renewable power supply using grid-connected vehicles - A 2030 case study for California and Germany, Applied Energy 2013; 104: 666-682.
[131] Tovilović, D. M. Rajaković, N. L. J., The simultaneous impact of photovoltaic systems and plug-in electric vehicles on the daily load and voltage profiles and the harmonic voltage distortions in urban distribution systems, Renewable Energy 2015: 76; 454-464.
[132] Ashtari, A., Bibeau, E., Shahidinejad, S., Molinski, T., PEV Charging Profile Prediction and Analysis Based on Vehicle Usage Data, IEEE Transactions on Smart Grid 2012; 3: 341-350.
[133] Clement-Nyns, K., Haesen, E., Driesen, J., The Impact of Charging Plug-In Hybrid Electric Vehicles on a Residential Distribution Grid, IEEE Transactions on Power Systems 2010; 25:371-380.
[134] Dallinger, D., Krampe, D., Wietschel, M., Vehicle-to-Grid Regulation Reserves Based on a Dynamic Simulation of Mobility Behavior, IEEE Transactions on Smart Grid 2011:2; 302-313.
[135] Darabi, Z., Ferdowsi, M., Aggregated Impact of Plug-in Hybrid Electric Vehicles on Electricity Demand Profile, IEEE Transactions on Sustainable Energy 2011; 2: 501-508.
[136] Deilami, D., Masoum, A. S., Moses, P. S., Masoum, M. A. S., Real-Time Coordination of Plug-In Electric Vehicle Charging in Smart Grids to Minimize Power Losses and Improve Voltage Profile, IEEE Transactions on Smart Grid 2011; 2: 456-467.
[137] Pieltain Fernández, L.,Román, T. G. S., Cossent, R., Domingo, C. M., Frías, P., Assessment of the Impact of Plug-in Electric Vehicles on Distribution Networks, IEEE Transactions on Power Systems 2011; 26: 206-213.
[138] Lee, T-K., Adornato, B., Filipe, Z. S., Synthesis of Real-World Driving Cycles and Their Use for Estimating PHEV Energy Consumption and Charging Opportunities: Case Study for Midwest U.S., IEEE Transactions on Vehicular Technology 2011; 60: 4153-4163.
[139] Li, G.,Zhang, X-P., Modeling of Plug-in Hybrid Electric Vehicle Charging Demand in Probabilistic Power Flow Calculations, IEEE Transactions on Smart Grid 2012; 3: 492-499.
[140] Pashajavid, E., Golkar, M. A, Charging of plug-in electric vehicles: Stochastic modelling of demand with domestic grids, in proceedings of Iranian Conference

on Electrical Engineering, Teheran 15-17 May 2012; 535-539.
[141] Qian, K., Zhou, C., Allan, M., Yuan, Y., Modeling Load Demand Due to EV Battery Charging in Distribution Grid, IEEE Transactions on Power Systems 2011; 26: 802-801.
[142] Shahidinejad, S., Filizadeh, S., Bibeau, E., Profile of Charging Load on the Grid Due to Plug-in Vehicles, IEEE Transactions on Smart Grid 2012; 3: 135-141.
[143] Soares, F. J., Peças-Lopez, J. A., Almeida, P. M. R., Moreira, C. L., Seca, L., A Stochastic Model to Simulate Electric Vehicles Motion and Quantify the Energy Required From the Grid, in Proceedings of the 17th Power Systems Computer Conference, Stockholm, Aug. 22-26, 2011.
[144] Trovão, L., Jorge, H. M., Power Demand Impacts of the Charging of Electric Vehicles on the Power Distribution Network in a Residential Area, in proceedings of the 2011 3rd International Youth Conference on Energetics, 7-9 July Leiria, 2011; 1-6.
[145] Zhang, H., Tang, W., Hu, Z., Song, Y., Xu, Z., Wang, L., A Method for Forecasting the Spatial and Temporal Distribution of PEV Charging Load, In proceedings of PES General Meeting 27-31 July at National Harbour, USA, 2014.
[146] Grahn, P., Alvehag, K.., Söder L., PHEV Utilization Model Considering Type-of-Trip and Recharging Flexibility, IEEE Transactions on Smart Grid 2014: 5; 139-148.
[147] Lojowska, A., Kurowicka, D., Papeafthymiou, D. , van der Sluis, L., Stochastic Modeling of Power Demand Due to EVs Using Copula, IEEE Transactions on Power Systems 2012; 27: 1960-1968.
[148] Lojowska, A., Kurowicka, D., Papaefthymiou, G., van der Sluis, L., From transportation patterns to power demand: Stochastic modeling of uncontrolled domestic charging of electric vehicles, IEEE Power and Energy Society General Meeting, San Diego 24-29 July 2011; 1-7.
[149] Papaefthymiou, G., Kurowicka, D., Using Copulas for Modeling Stochastic Dependence in Power System Uncertainty Analysis, IEEE Transactions on Power Systems 2009; 24: 40-49.
[150] Rychlik, I., Rydén, J., Probability and Risk Analysis. An Introduction for Engineers, Springer-Verlag 2006.
[151] Lai, C.-D., Murthy, D. N., Xie, M., Weibull Distributions and Their Applications, Springer Handbook of Engineering Statistics, Ed. P. Hoang Springer-Verlag 2006; 63-78.
[152] Abramowitz, M., Stegun, I. A., Handbook of Mathematical Functions with Formulas, Graphs, and Mathematical Tables, New York: Dover 1965.
[153] Beaulieu, N. C., Abu-Dayya, A. A., McLane, P. J., Estimating the distribution of a sum of independent log-normal random variables, IEEE Transactions on Communications 1995; 43: 2869- 2873.
[154] Nadarajah, S., A Review of Results on Sums of Random Variables, Acta Applicandae Mathematicae 2008; 103: 131-140.
[155] Titterington, D. M., Smith, A. F., Makov, U. E., Statistical Analysis of Finite Mixture Distributions, Wiley, Chapter 3.3, 1985.
[156] Pawitan, Y., In All Likelihood: Statistical Modelling and Inference Using

Likelihood. Oxford University Press, 2001.
[157] Mann, N. R., Fertig, K. W., A Goodness-of-Fit Test for the Two Parameter vs. Three-Parameter Weibull; Confidence Bounds for Threshold, Technometrics 1975; 17: 237-245.
[158] Swedish Meteorological and Hydrological Institute, Data set on solar irradiation for Norrköping 2013, SMHI database 2013.
[159] Ineichen, P., Perez, R., A new airmass independent formulation for the Linke turbidity coefficient, Solar Energy 2002: 73; 151-157.
[160] Benaglia, T., Chauveau, D., Hunter, D. R., Young, D. S., mixtools: An R package for analyzing mixture models, Journal of Statistical Software 2009: 32; 1-29.
[161] Marcos, J., Marroyo, L., Lorenzo, E., García, M., Smoothing of PV power fluctuations by geographical dispersion, Progress in Photovoltaics: Research and Applications 2012: 20; 226-237.
[162] Lave, M., Kleissl, J., Arias-Castro, E., High-frequency irradiance fluctuations and geographic smoothing, Solar Energy 2013: 86; 2190-2199.
[163] Perpiñínan, O., Marcos, J., Lorenzo, E., Electrical power fluctuations in a network of DC/AC inverters in a large PV plant: Relationship between correlation, distance and timescale, Solar Energy 2013: 88; 227-241.
[164] Widén, J., Modelling and statistical analysis of the variability of large-scale solar power in high-latitude power systems, in Proceedings of the 1st International Workshop on Integration of Solar Power into Power Systems, Aarhus, Denmark, 2011.
[165] Suehrcke, H., 2000, On the relationship between duration of sunshine and solar radiation on the earth's surface: Ångströms equation revisited, Solar Energy 2000: 68; 417-425.
[166] Dervishi, S., Mahdavi, A., Computing diffuse fraction of global horizontal solar radiation: A model comparison, Solar Energy 2012: 86; 1796-1802.
[167] Erbs, D. G., Klein, S. A., Duffie, J. A., Estimation of the diffuse radiation fraction for hourly, daily and monthly-average global radiation, Solar Energy 1982: 28; 293-302.
[168] Duffie, J. A., Beckman, W. A., Solar Engineering of Thermal Processes, 3rd Ed., Hoboken, NJ: Wiley, 2006.
[169] King, D. L., Gonzales, S., Galbraith, G. M.,Boyson, W. E., Performance model for grid-connected photovoltaic inverters, Report No.: SAND2007-5036, Sandia National Laboratories, Albuquerque, 2007.
[170] Meteonorm, `www.meteonorm.com`, (Retrieved 2015-01-08).
[171] Carpenato, E., Chicco, G., Probabilistic characterisation of the aggregated residential load patterns, IEEE Generation, Transmission & Distribution, IET 2008; 2: 373-382.
[172] Statistics Sweden, Time Use Diaries Pilot Study, 1996.
[173] Gut, A., An Intermediate Course in Probability, Springer-Verlag, 2009.
[174] Kimball, H. H., Variations in the total and luminous solar radiation with geographical position in the United States, Monthly Weather Review 1919: 47; 769-793.
[175] Prescott, J. A., Evaporation from a water surface in relation to solar radiation, Transactions of the Royal Society of Australia 1940: 64; 114-118.

[176] Knutsen, D., Willén O., A study of electric vehicle charging patterns and range anxiety, UPTEC Report, STS13, 2013.
[177] The GeoInformation Group, UKMap, GIS Database 2014, `http://www.geoinformationgroup.co.uk/products/ukmap`, (Retrieved 2015-01-08).
[178] City of Westminster, Westminster Population, `http://www.westminster.gov.uk/westminster-population`, 2013, (Retrieved 2015-01-08).
[179] Office for National Statistics, Neighborhood Statistics, `http://www.neighbourhood.statistics.gov.uk/`, (Retrieved 2015-01-08).

Acta Universitatis Upsaliensis

Digital Comprehensive Summaries of Uppsala Dissertations from the Faculty of Science and Technology 1224

Editor: The Dean of the Faculty of Science and Technology

A doctoral dissertation from the Faculty of Science and Technology, Uppsala University, is usually a summary of a number of papers. A few copies of the complete dissertation are kept at major Swedish research libraries, while the summary alone is distributed internationally through the series Digital Comprehensive Summaries of Uppsala Dissertations from the Faculty of Science and Technology. (Prior to January, 2005, the series was published under the title "Comprehensive Summaries of Uppsala Dissertations from the Faculty of Science and Technology".)

Distribution: publications.uu.se
urn:nbn:se:uu:diva-243159

ACTA
UNIVERSITATIS
UPSALIENSIS
UPPSALA
2015